Project Deliverable D1.4

Wildfire water and economic impact assessment, focussed on forest land loss and Portuguese water quality

Call / Topic	H2020-MSCA-ITN-2019
Project Acronym	PYROLIFE
Project Title	Training the next generation of integrated fire management expertsm
Project Number	860757
Project Start Date	01/10/2019
Project Duration	63 months
Contributing WP	WP 1
Dissemination Level	Public
Contractual Delivery Date	Month 40 (31/01/2023)
Actual Delivery Date	31/01/2023
Contributors	Sarah Meier (University of Birmingham) Eric Strobl (University of Bern) JRobert J. R. Elliott (University of Birmingham) Nicholas Kettridge (University of Birmingham)

Document History

Version	Date	Modifications	Source
1.0	31/01/2023	Final version submitted to the portal	EUC

Preamble to this deliverable

This deliverable concerns an analysis of economic impacts of fire. The analysis on the impact of fire on Portuguese water quality will be submitted as an additional deliverable with a deadline in May 2024.

DOI: 10.1111/risa.14075

ORIGINAL ARTICLE

Cross-country risk quantification of extreme wildfires in Mediterranean Europe

Sarah Meier[1] | **Eric Strobl**[2] | **Robert J. R. Elliott**[3] | **Nicholas Kettridge**[1]

[1]School of Geography, Earth and Environmental Sciences, University of Birmingham, Birmingham, West Midlands, United Kingdom

[2]Department of Economics, University of Bern, Bern, Bern, Switzerland

[3]Department of Economics, University of Birmingham, Birmingham, West Midlands, United Kingdom

Correspondence
Sarah Meier, School of Geography, Earth and Environmental Sciences, University of Birmingham, Edgbaston, Birmingham B15 2TT, United Kingdom.
Email: meier.sar@gmail.com

Funding information
H2020 Marie Skłodowska-Curie Actions, Grant/Award Number: 860787

Abstract

We estimate the country-level risk of extreme wildfires defined by burned area (BA) for Mediterranean Europe and carry out a cross-country comparison. To this end, we avail of the European Forest Fire Information System (EFFIS) geospatial data from 2006 to 2019 to perform an extreme value analysis. More specifically, we apply a point process characterization of wildfire extremes using maximum likelihood estimation. By modeling covariates, we also evaluate potential trends and correlations with commonly known factors that drive or affect wildfire occurrence, such as the Fire Weather Index as a proxy for meteorological conditions, population density, land cover type, and seasonality. We find that the highest risk of extreme wildfires is in Portugal (PT), followed by Greece (GR), Spain (ES), and Italy (IT) with a 10-year BA return level of 50'338 ha, 33'242 ha, 25'165 ha, and 8'966 ha, respectively. Coupling our results with existing estimates of the monetary impact of large wildfires suggests expected losses of 162–439 million € (PT), 81–219 million € (ES), 41–290 million € (GR), and 18–78 million € (IT) for such 10-year return period events.

KEYWORDS
environmental economics, environmental hazards, extreme value statistics, risk analysis, wildfires

SUMMARY

We model the risk of extreme wildfires for Italy, Greece, Portugal, and Spain in form of burned area return levels, compare them, and estimate expected losses.

1 | INTRODUCTION

Wildfires affect humans, assets, and ecosystems and can lead to extensive socioeconomic and environmental impacts (Keeley et al., 2012). Within Europe, the Mediterranean region is the most fire prone with high wildfire incidence and consequences (San-Miguel-Ayanz et al., 2020). This was bleakly illustrated by the pronounced wildfire season in 2017 with blazing fires in France and roughly 140'000 hectares (ha) burnt in Portugal (NATURE, 2017), or by the 2018 fatal fires in Greece leading to more than 100 deaths and causing major damage to the ecosystems of the susceptible *Natura 2000* protected areas (San-Miguel-Ayanz et al., 2018). Not only do Portugal (PT), Spain (ES), Italy (IT), Greece (GR), and France (FR) combined account for about 85% of the total annual burned area (BA) in Europe (De Rigo et al., 2017), the Mediterranean area is also particularly vulnerable in that it is densely populated, characterized by a large wildland–urban interface (WUI) (San-Miguel-Ayanz et al., 2013), and due to the species richness as well as the high proportion of endemisms, it marks a "biodiversity hotspot" (Batllori et al., 2013; Myers et al., 2000).

Notably, fire has historically played an integral role in Mediterranean Europe by performing highly beneficial ecosystem functions (Holmes et al., 2008), and has been utilized by communities for agricultural practices (e.g., to

fertilize soils and control plant growth) and landscape modifications (Santín & Doerr, 2016). However, although societies and ecosystems are likely to adapt to near-normal conditions, this is arguably not the case for extreme events (Bowman et al., 2017; San-Miguel-Ayanz et al., 2013; Tedim et al., 2018). Rather, evidence shows that particularly large wildfires are linked to severe disturbances and losses and are the cause of the bulk of social, economic, and adverse environmental impacts (Evin et al., 2018; Gill & Allan, 2008; Mendes et al., 2010).

The purpose of this study is to characterize the spatiotemporal distribution and dynamics of extremely large wildfires in Mediterranean Europe, as well as to quantify and compare their risk probabilities across countries. Since our interest lies in the risk quantification of rare or extreme events, we model the probabilistic structure of the commonly heavy-tailed right tail of the wildfire BA density distribution (Beverly & Martell, 2005; Hernandez et al., 2015; Scotto et al., 2014) applying extreme value theory (EVT). A series of commonly known variables that potentially influence the production of large wildfires, such as the Fire Weather Index (FWI), population density, land cover type, and seasonality, are included as covariates to evaluate potential conditional probabilities. Employing the analytical tools provided by EVT enables to extrapolate wildfires of potentially unobserved size based on the European Forest Fire Information System (EFFIS) BA data set from 2006 to 2019, and thus, to quantify the risk of country-level extreme wildfires. Furthermore, we convert our estimates into rough monetary losses using figures from the existing literature to facilitate the potential application of our estimates to policy decisions.

EVT has been proven to be a suitable inferential tool for wildfire size risk quantification (Hernandez et al., 2015; Holmes et al., 2008), and has been applied globally (Jiang & Zhuang, 2011; Keyser & Westerling, 2019). For Mediterranean Europe, Evin et al. (2018) evaluate the risk of large wildfires in France conditional on a new fire policy introduced in 1994. Moreover, several studies quantify and compare regional wildfire risk and regimes in Portugal (De Zea Bermudez et al., 2009; Mendes et al., 2010; Scotto et al., 2014), which is unsurprising given the country bears the highest wildfire prevalence within Mediterranean Europe (Turco et al., 2019). However, to the best of our knowledge, ours is the first study to use EVT to perform a cross-country quantification of wildfire risk. Our contribution is threefold. First, we merge high-quality homogenized and up-to-date geospatial data sets for the European Mediterranean region. Second, we perform a country-level analysis of extremely large wildfires in Mediterranean Europe, and third, we compare the estimated risks across the region.

The remainder of this study is organized as follows. Section 2 describes the data sources followed by Section 3 outlining the methodology underpinning the extreme value analysis. Section 4 summarizes the results and derives monetary losses by matching our estimates with economic loss figures from the existing literature. The findings are subsequently discussed in Section 5, before Section 6 concludes.

2 | DATA AND VARIABLES

2.1 | Burned area

We use a high-quality BA spatial data product compiled by the Joint Research Centre (JRC) and provided by the EFFIS.[1] It is the primary source of harmonized data on wildfires in Europe, and thus enables a sound cross-country comparison. The data product is derived from semiautomatic classification of daily processing of Moderate Resolution Imaging Spectroradiometer (MODIS) satellite imagery at 250 m spatial resolution. The definite fire perimeters are refined through visual image interpretation and systematically collected fire news from various media. The data set includes fires larger than approximately 30 ha, and contains information on the initial date, country, province, place, as well as the BA polygons.[2] We model the extreme BA conditional on the covariates described hereafter. For the full list of covariates refer to Table A1 in Appendix A in the Supporting Information.

2.2 | Fire Weather Index

Weather conditions are a major driver of wildfire events and are commonly applied to construct fire danger indices (Bedia et al., 2014; Krawchuk et al., 2009; Sousa et al., 2015). We employ the FWI component of the Canadian Forest Fire Weather Index System as a proxy for meteorological conditions incorporating temperature, wind speed, relative humidity, and precipitation. Providing a homogeneous numerical rating of relative fire potential resulting from the combination of the two fire behavior indices, namely, the Buildup Index and the Initial Spread Index (Van Wagner & Pickett, 1985), the FWI has become a reference index for European fire danger maps produced by the JRC (Camia et al., 2008). We use a high-resolution calculation developed by Natural Resources Canada based on the European Centre for Medium-Range Weather Forecasts ERA5-HRES[3] reanalysis product presented in McElhinny et al. (2020). To account for the effect of interseasonal drought, we use the FWI version derived from the overwintered Drought Code with a spatial resolution of 31 km (0.28° on a reduced Gaussian grid).

We spatially join the centroid of every wildfire polygon to the closest grid cell of the FWI data set and extract (i) the daily FWI values 1 month prior, as well as 1 week after the initial date of the fire, and (ii) the daily FWI values of the respective year of the fire. Using (i), we create the variables FWI on the initial date (*FWI_InitDat*), the mean FWI of the month prior to the initial date (*FWI_MP*), the mean FWI of the week prior to the initial date (*FWI_WP*), and the mean FWI of the month prior until the week after the initial

[1] https://effis.jrc.ec.europa.eu.
[2] https://effis.jrc.ec.europa.eu/about-effis/technical-background/rapid-damage-assessment.
[3] https://cds.climate.copernicus.eu/cdsapp#!/home.

date (*FWI_MP_WA*). We employ (ii) to estimate the annual mean as well as the 0.5, 0.9, 0.95, 0.99 quantiles (*FWI_Mean*, *FWI_q*0.5, *FWI_q*0.9, *FWI_q*0.95, *FWI_q*0.99) of the FWI for the corresponding year of the fire incidence.

2.3 | Population density

Population density has gained widespread attention for its role as an ignition source, as a facilitator of suppression efforts, and as a factor that captures impact-related importance (Fernandes, 2019; González-Cabán, 2009; Lankoande & Yoder, 2006; Pechony & Shindell, 2010). To proxy population density near wildfires, we use the Oak Ridge National Laboratory's *LandScan*[4] annual global population distribution data provided at approximately 1 km (30'') spatial resolution. The raster data representing the ambient population distribution are based on remote sensing imagery analysis techniques, and demographic and geographic data. We create approximately 4 km buffers[5] around the centroid of the polygons and calculate the mean population density in counts per square kilometer of the respective *LandScan* year denoted by the variable *Pop_4km*.

2.4 | Land cover type

The 2006, 2012, and 2018 versions of the Copernicus' CORINE land cover[6] are employed to categorize the EFFIS perimeters of BA to evaluate a potential correlation between land cover type and the distribution of large fires. The CORINE land cover information is derived from satellite data[7] using a minimum mapping unit of 25 ha and consists of an inventory of 44 land cover classes. We extract the dominant land cover type for each EFFIS BA polygon considering the latest version of the CORINE land cover data with respect to the initial date of the observation. We further reclassify the most prevalent land cover types for each country with regard to the extreme wildfire observations. For an overview of the dominant land cover types for each country, see Table A2 of Appendix A in the Supporting Information. In the conducted analysis, types I to III are incorporated as indicator variables. A fourth indicator variable named *Type_Other* is created where none of the three types applies.

3 | METHODS

3.1 | Point process (PP) using maximum likelihood estimation

The foundation of the PP approach regarding extremal processes was originally introduced by Pickands (1971), and applied to environmental processes by Smith (1989). The PP approach is particularly suitable as it uses data efficiently and can easily be adapted to include temporal or covariate effects (Coles, 2001). We apply a nonhomogeneous PP model to simulate the occurrence (i.e., frequency of exceedance) and intensity (i.e., excess) of a value of BA above a chosen threshold.

Let X_i be a series of independent and identically distributed (i.i.d.) random variables representing wildfire BAs, and $N_n = \{(\frac{i}{n+1}, X_i) : i = 1, n\}$ be a sequence of PPs. Then, given a sufficiently large threshold u, on regions of the form $[0,1] \times (u, \infty)$, the PP N_n is approximately a Poisson process with the intensity measure $\Lambda(A)$ shown in Equation (1) on a set of the form $A = [t_1, t_2] \times (u, \infty)$:

$$\Lambda(A) = n_y(t_2 - t_1)\left(1 + \xi\left(\frac{u-\mu}{\sigma}\right)\right)^{-1/\xi}. \quad (1)$$

The interval (t_1, t_2) on the abscissa is a subset of [0,1] and n_y denotes the number of years of observations so that events in nonoverlapping subsets of $[0,1] \times (u, \infty)$ are independent and the estimated parameters ξ, μ, and σ correspond to the generalized extreme value (GEV) distribution. It envelops three types of limit distributions, which are uniquely defined by the shape parameter ξ. The Fréchet distribution ($\xi > 0$) is characterized by a heavy tail, the Gumbel distribution ($\xi = 0$) exposes an exponential decay of the tail, whereas a Weibull limit distribution ($\xi < 0$) has an upper bound. In general, a heavier tail implies that the probability of an "unexpected" event is larger, while the location μ and the scale σ parameters relate to the mean and spread of the distribution, respectively. For greater detail on the GEV see Appendix B in the Supporting Information.

Following Coles (2001), the model parameters are estimated by maximizing the likelihood function

$$L(\mu, \sigma, \xi) = \exp\left\{-n_y\left[1 + \xi\frac{u-\mu}{\sigma}\right]^{-1/\xi}\right\} \times \prod_{i=1}^{N(A)} \sigma^{-1}\left\{\left[1 + \xi\left(\frac{x_i - \mu}{\sigma}\right)\right]^{-\frac{1}{\xi}-1}\right\}^{\delta_i[x_i > u]}, \quad (2)$$

where δ_i is one if the realization of $X_i > u$, and zero otherwise. The first part of the likelihood expression entails the contribution of the number of fire events (occurrence) characterized by the Poisson distribution with mean $\Lambda\{[0,1] \times [u, \infty)\}$. The second part shows the excess contribution of the observations (intensity), which are modeled as generalized Pareto distribution (GPD). σ is adjusted as $\sigma^* = \sigma(u) - \xi u$, so that the scale parameter is independent of the threshold. The cumulative GPD is given by Equation (3):

$$F(z; \sigma^*, \xi, u) = \begin{cases} 1 - \left[1 + \xi(\frac{z-u}{\sigma^*})\right]^{\frac{-1}{\xi}}, & \text{for } \xi \neq 0 \\ 1 - e^{\frac{-z}{\sigma^*}}, & \text{for } \xi = 0, \end{cases} \quad (3)$$

where $1 + \xi(\frac{z-u}{\sigma^*}) > 0$, $z - u > 0$, and $\sigma^* > 0$.

[4] https://landscan.ornl.gov.
[5] The exact measure is 0.05 decimal degrees, which at 45°N corresponds to 3'935.5 m.
[6] https://land.copernicus.eu/pan-european/corine-land-cover.
[7] 2006: SPOT-4/5 and IRS P6 LISS III; 2012: IRS P6 LISS III and RapidEye; 2018: Sentinel-2 and Lansat-8.

Given that X has a GPD, the distribution of the rescaled random variable z/σ^* is independent of σ^* (Katz et al., 2005).

We perform the numerical optimization using the R package *extRemes* (Gilleland & Katz, 2016) to estimate Equation (2).

3.2 | Model assumptions

The theoretical justification for using a PP characterization of extremes is predicated on the assumptions of (i) unbiased threshold choice, (ii) stationarity, and (iii) independence of the excesses. Regarding (i), too low a threshold leads to a bias potentially violating the asymptotic basis of the model. If the threshold chosen is too high, the reduction of data points leads to high variance. We determine the individual countries' thresholds using the threshold diagnostic tools provided in the R package *extRemes*. They are based on the following rationale. Let the excesses over a threshold u be defined as $y = x - u$. Recalling from Section 3.1 that these excesses follow a GPD, this also holds true for all $y > 0$ of a threshold $v > u$ with

$$GPD\big(y, \sigma_v, \xi_v\big) = \frac{GPD\big((v-u)+y, \sigma_u, \xi_u\big)}{GPD\big((v-u), \sigma_u, \xi_u\big)}. \tag{4}$$

As a consequence, Equation (4) can only be satisfied if $\xi_v = \xi_u$ and $\sigma_v - \xi \cdot v = \sigma_u - \xi \cdot u$. This implies that for a sufficiently high threshold, both the shape parameter ξ and the modified scale $\sigma - \xi u$ are independent of the threshold and need to be stable. Besides plotting the shape and modified scale parameters individually, the mean value of the excesses y over u can be plotted against u, which is known as the Mean Residual Life (MRL) plot (Coles, 2001). The GPD is deemed to fit the data well when a straight line starting from the selected threshold can be fitted within the confidence bands of the MRL plot, and thereby indicating a stable distribution. In practice, the visual interpretation of the MRL plot, as well as the individual parameter plots, is somewhat subjective. Thus, we additionally consider the threshold selection suggestions provided by the automated Bayesian leave-one-out cross-validation approach, which compares the extreme value predictive performance resulting from each of a set of thresholds. This approach was first introduced by Northrop et al. (2017) and is implemented in the R package *threshr* (Northrop & Attalides, 2020). As this approach is only applicable for independent observations, we compare outcomes in an iterative process with the estimation of the extremal index θ as a measure of dependence.

While Equation (2) implicitly assumes stationarity of the GEV parameters, we also estimate nonstationary models where ξ, μ, and σ are conditioned on various functional forms of the covariates described in Section 2 (as well as on seasonality variables) in order to assess assumption (ii). Equation (5) serves as an example of modeling a nonconstant linear location parameter dependent on the mean FWI of the month prior to the initial date *FWI_MP*:

$$\mu(FWI\_MP) = \mu_O + \mu_1 * FWI\_MP. \tag{5}$$

The evaluation of the nonstationary models is based on the Akaike information criterion (AIC), the Bayesian information criterion (BIC), and, for nested models, on the likelihood ratio test.[8] We systematically model the location, shape, and scale parameters individually and combined starting with linear functional forms of the respective parameters. Whenever a model shows an improvement over the stationary model, we explore more complex functional forms (i.e., quadratic and interactions). In cases where the parameter confidence intervals (CIs) could not be estimated via the delta method, 500 iterative bootstraps with replacement were applied to evaluate the parameter significance.

As a means to examine the independence assumption (iii), the degree of dependence is explored using the extremal index $\theta \in (0, 1]$ suggested by Ferro and Segers (2003), which is defined as:

$$\theta = \begin{cases} \min\left\{1, \frac{2\left(\sum_{i=1}^{N-1} T_i\right)^2}{(N-1)\sum_{i=1}^{N-1} T_i^2}\right\}, & \text{if } \max\{T_i : 1 \le i \le N-1\} \le 2 \\ \min\left\{1, \frac{2\left(\sum_{i=1}^{N-1} (T_i-1)\right)^2}{(N-1)\sum_{i=1}^{N-1} (T_i-1)(T_i-2)}\right\}, & \text{if } \max\{T_i : 1 \le i \le N-1\} > 2, \end{cases} \tag{6}$$

where T_i denotes the length between excesses (interexceedance time). A value of the extremal index $\theta = 1$ implies complete independence, whereas $\theta \to 0$ indicates perfect dependence. In case the extremal index suggests a violation of the independence assumption, the data can be declustered to filter the dependent observations.

3.3 | Model fit

In order to assess the fit of the selected model, we implement two common diagnostic plots incorporated in the *extRemes* package. First, we avail of the Z-plot following Smith and Shively (1995). Let Zk be the Poisson intensity parameter integrated from exceedance time $k-1$ to exceedance time k (starting the series with $k = 1$). The Z-plot then determines whether this random variable Zk is independent exponentially distributed with mean one, which corresponds to the observations lying on the diagonal. Second, we plot the kernel density functions of the observed data versus the modeled distribution. For the particular case of the PP characterization of extremes, the density of the calculated data block maxima is compared to the PP model with respect to the equivalent GEV.

[8] Suppose that the negative likelihood is x for the stationary base model and y for the restricted model, the deviance statistic $D = -2(y - x)$ then follows the χ_k^2 distribution, where k indicates the difference in the number of estimated parameters (Coles, 2001).

3.4 | Return levels (quantiles)

Harnessing the estimated probabilities associated with extremes, the interest is typically focused on providing estimates of the upper quantiles of the modeled distribution functions. Specifically, the return level of an extremely large fire, defined as z_p, which is associated with a return period of $1/p$, embodies a tangible outcome. It is equivalent to the $(1-p)$th quantile of the corresponding modeled distribution by the PP representation of extremes. As the PP approach combines the Poisson distribution parameter with the GPD, the return level z_p is obtained by setting the cumulative distribution function Equation (3) equal to the desired quantile $1-p$. Solving for z (for a probability p) leads to Equation (7) (Coles, 2001):

$$z_p = F^{-1}\left(1-p;\sigma^*,\xi,u\right) = \begin{cases} u+(\sigma^*/\xi)\left(p^{-\xi}-1\right), & \text{for } \xi \neq 0 \\ u+\sigma^* \ln(1/p), & \text{for } \xi = 0, \end{cases} \quad (7)$$

where the return level z_p denotes the BA level that is expected to be exceeded in any given year with probability p.

3.5 | Economic valuation

A transformation of the informational content of the BA return-level estimates into economic values could arguably be beneficial supporting policy decisions. Our approach in this regard is to multiply associated per ha monetary losses with the expected BA, as suggested by Holmes et al. (2008). To this end, we resort to existing studies either providing explicit per ha loss estimates or we calculate per ha values by combining information on total BA with total loss estimates. To facilitate a comparison over space and time, spatial values are harmonized in hectares, and monetary values are inflation adjusted and expressed in 2020 euros using the 2020 monthly average exchange rate (US$ = 0.87€). Values in U.S. dollars are deflated based on the not seasonally adjusted urban Consumer Price Index CPI.[9] Table 1 provides a summary of the economic impact aspects that have been included in each study as well as of the inflation-adjusted €per ha monetary values for the five papers included in the table. Note that the calculated €/ha losses are highly dependent on the estimation method used, the type of damage and losses included, and on the specific situation of the fire (season) that is studied in the article. Therefore, the figures derived from the multiplication of our return levels with estimates from existing publications need to be interpreted with caution.

More specifically, two studies have a European context. The first estimates we derive are from a comprehensive report for Mediterranean forests by Merlo and Croitoru (2005), who provide figures in 2001 prices that encompass country-specific estimates of 884€/ha (GR), 1'480€/ha (IT), and 3'420€/ha (PT). This translates into inflation-adjusted monetary values expressed in 2020 euros of 1'228€/ha (GR), 2'004€/ha (IT), and 4'728€/ha (PT). We also include the economic impact estimates from a study of Galicia, Spain, by Barrio et al. (2007), which implements an ecosystem service approach based on assessing services that are affected due to wildfire existence. The reported monetary losses range from 2'249 to 3'162 €/ha in 2006 values. We apply the mean of this range, that is, 3'304€/ha in 2020 euros.

As suitable research on Southern Europe is limited, we also include three loss estimates derived from studies of U.S. wildfires. The Butry et al. (2001) case study assesses the Florida 1998 summer wildfires that burned a total of around 500'000 acres (202'343 ha). We apply the conservative lower bound total cost estimate of US$ 600 million (in 2001 values). Dividing the total cost by the total BA leads to an inflation-adjusted estimate of 3'801€/ha. A second study by Rahn et al. (2014) evaluates the 2003 wildfires in San Diego (United States) and reports a cost of US$ 6'500 per acre (US$ 2'630/ha in 2014 values), which is equivalent to 3'230€/ha in 2020 euros. Finally, we include the recent publication on California wildfires by Safford et al. (2022), who investigate the extraordinary 2020 fire season. The authors estimate losses of US$ 19 billion for a historical record of 1.74 million ha BA, which is equivalent to 8'717€/ha in 2020 euros.[10]

4 | RESULTS

4.1 | Summary statistics

Country-level BA summary statistics of the EFFIS BA data product are presented in Table 2. The single largest fire in the data set that burnt 67'521 ha occurred in October 2017 in Portugal. Greece exhibits a comparably lower frequency of fires but has the largest mean, median, 75 percentile, and 90 percentile BA values. The highest annual wildfire incidence is recorded in Italy.

Figure 1 presents the log transformed wildfire BA observations from 2006 to 2019 at the country level. The data show a slightly decreasing tendency in BA for Spain, France, Italy, and Greece, and no clear trend in Portugal. However, a slightly different picture emerges from Figure A1 of Appendix A in the Supporting Information when we focus on BA extremes, herein defined as the wildfires that exceed the selected country-level threshold. While, once again, we observe decreasing BA trends for France, Italy, and Greece,

[9] https://www.bls.gov/cpi.

[10] Extensive research conducted by Wang et al. (2021) estimates the economic losses for the 2018 wildfire season in California that include indirect losses and suggests total wildfire damages were in the region of US$148.5 billion for a total BA of 7'700 km^2. This leads to a per ha loss estimate of 165'467 €/ha in 2020 euros, which is around 19 times larger than the Safford et al. (2022) estimate for the 2020 season. Given this estimate is far beyond all the other estimates, we do not use it in this analysis and only present the more conservative estimates. However, Wang et al. (2021) give some indication of how far reaching the costs of extreme wildfires are when we include indirect health costs as well as costs arising outside the affected region assuming extreme fires in Mediterranean Europe are comparable to those in California.

TABLE 1 Included economic impacts and €/ha economic loss estimates in 2020 euros

Barrio et al. (2007)	**Butry et al. (2001)**	**Merlo and Croitoru (2005)**	**Rahn et al. (2014)**	**Safford et al. (2022)**
Country (region)				
Spain (Galicia)	**United States (Florida)**	**Portugal, Italy, Greece**	**United States (San Diego)**	**United States (California)**
Economic impacts considered				
Ecosystem service approach	**Seven categories**	**Direct losses due to forest fires**	**Five categories**	**Ecological and socioeconomic evaluation**
• goods and services[h]	• insured property damage	• wood losses	• state/agency[d]	• structures lost
• negative externalities[e]	• pine timber market long-run damage	• restoration costs	• infrastructure[i]	• property damage
• property damage	• presuppression costs[c]		• natural areas[g]	• lives lost
• suppression costs	• tourism-related costs		• business[b]	• suppression cost
	• suppression costs		• community[j]	• ecosystem impact[a]
	• disaster relief expenditures			
	• human health effects[f]			
€/ha loss estimates				
3'304€	3'801€	PT: 4'728€	3'230€	8'717€
		ES: -		
		IT: 2'004€		
		GR: 1'228€		

[a]Defined in terms of tree mortality.
[b]Economic activity, employment impacts, building and property loss, tourism impacts.
[c]Including prescribed burning.
[d]Insurance implications, short- and long-term budget impacts, future resource impacts.
[e]Losses derived from CO^2 emissions.
[f]Short-run asthma-related healthcare costs.
[g]Species and habitats, erosion and flood control, watershed restoration, cultural and historic resources.
[h]Tourism, timber losses, CO_2 losses derived from biomass burned.
[i]Transportation repairs, water quality impacts, utilities replacement, communication repairs.
[j]Recreation impacts, health and human services, building and property loss, public assistance.

TABLE 2 BA summary statistics (2006–2019)

Country	n	Events per year (n_a)	Mean (ha)	Median (ha)	Pctl 75 (ha)	Pctl 90 (ha)	Max (ha)
Portugal	3'084	220.3	474	106	259	768	67'521
Spain	2'412	173.3	386	95	240	678	32'424
France	668	47.7	171	65	150	340	3'555
Italy	3'260	232.9	204	91	188	372	11'550
Greece	748	53.4	761	138	412	1'325	45'809

Note: n: number of observations; Pctl: percentile.

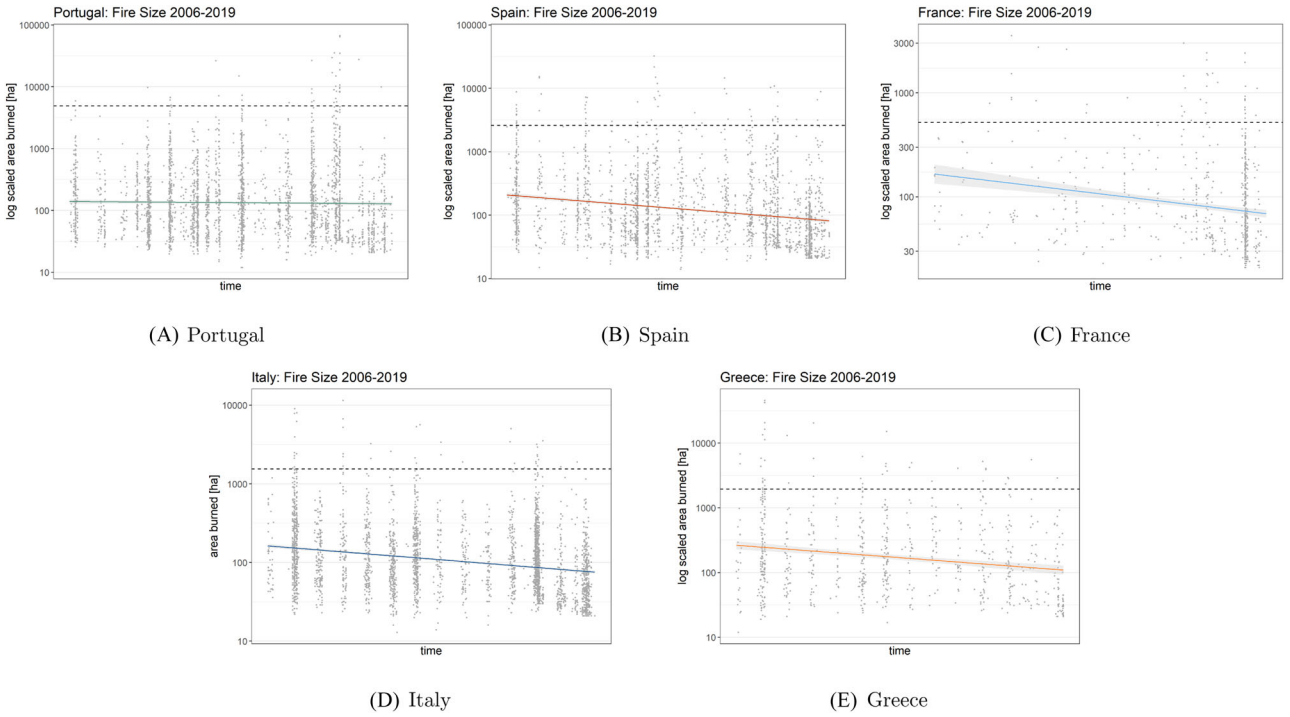

(A) Portugal (B) Spain (C) France

(D) Italy (E) Greece

FIGURE 1 BA (log_{10} scaled) with indicated threshold choice (black dashed line) over study period (2006–2019) with a generalized linear model smoothed conditional mean with CIs on the 90% level

no trend is evident for Spain. In contrast, the extreme BA values for Portugal exhibit an increasing trend, largely driven by the 2017 fire season.

Figure 2 displays the annual number of wildfires and total BA over the study period enabling a direct country comparison. There are few observations and little variation over the years for Greece, while the opposite is the case for Italy. The year 2017 particularly stands out for Portugal with many fire records as well as large total BA. For France, 2019 accounts for more than half of all the observations in the study period.

Regarding the correlation between BA and the covariates, there is a general tendency of a positive correlation between the BA and the mean FWI of the week prior to the fire initial date (*FWI_WP*). No conclusive relationship is observable between the BA and population density. Correlation plots are provided in the Supporting Information in Appendix A (Figure A2 and Figure A3 for the association of the FWI and the population density, respectively).

4.2 | Threshold selection/dependence test

The MRL plots with the final threshold choice (after considering all decision-supporting tools outlined in this section) are shown in Figure 3. Complementing the MRL plots, the individual behavior of the shape parameter ξ and the modified scale parameter $\sigma - \xi u$ are analyzed but not shown.

The Bayesian leave-one-out cross-validation plots are presented in Figure 4. These show a single run output and vary across different executions. The best threshold evaluated by this approach, denoted as u_b, is provided below the plot whenever it proved stable over 10 consecutive runs.

Table 3 provides a summary of the final threshold choices with the corresponding extremal indices θ, and the number of observations above the selected threshold. The excesses of Spain and Greece indicate perfect independence, while Portugal and Italy show a very high θ value. The lowest extremal index value is found for France, which did not improve after

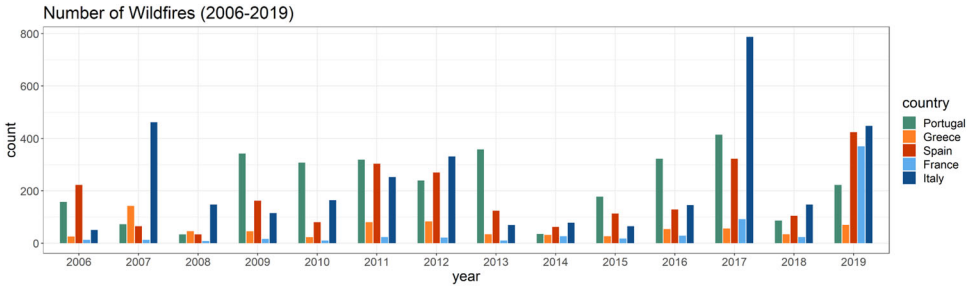

(A) Number of observations

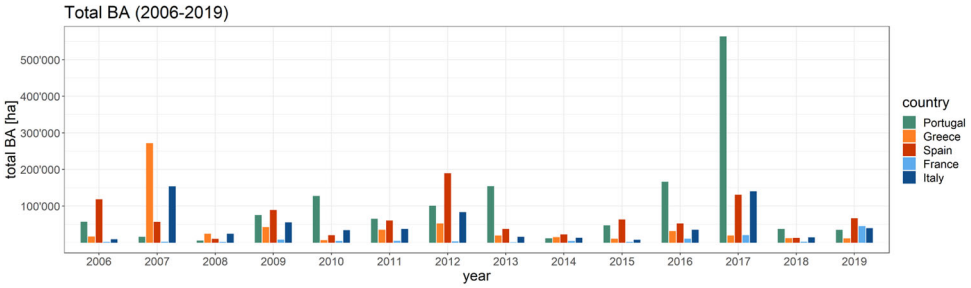

(B) Total BA

FIGURE 2 Annual number of wildfires and annual total BA in the EFFIS BA product

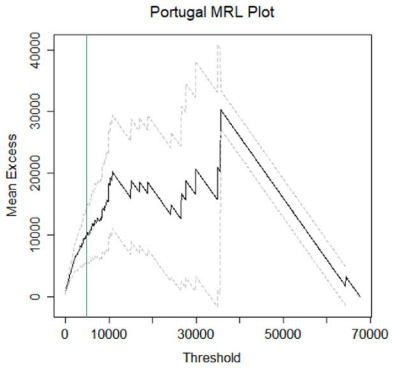

(A) Portugal $u = 4'900$ ha

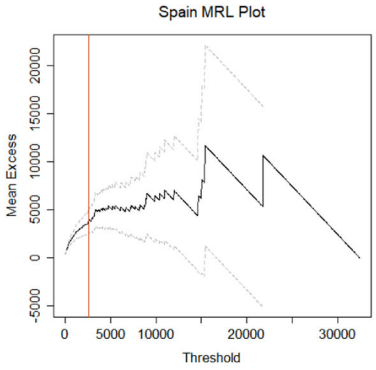

(B) Spain $u = 2'600$ ha

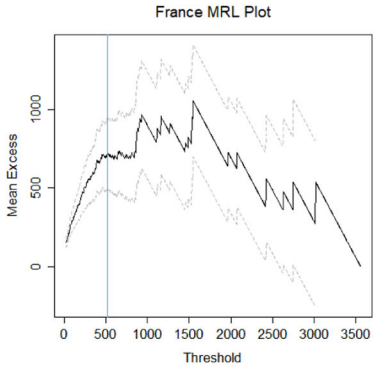

(C) France $u = 520$ ha

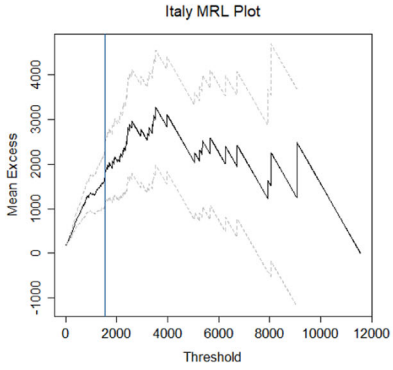

(D) Italy $u = 1'550$ ha

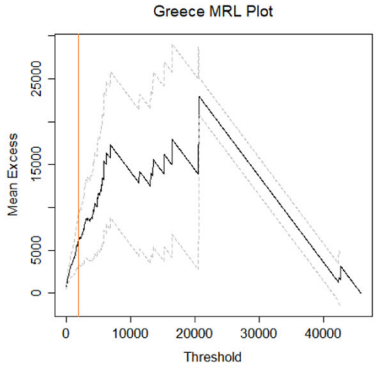

(E) Greece $u = 1'943$ ha

FIGURE 3 Mean Residual Life (MRL) plots with indicated final threshold choice

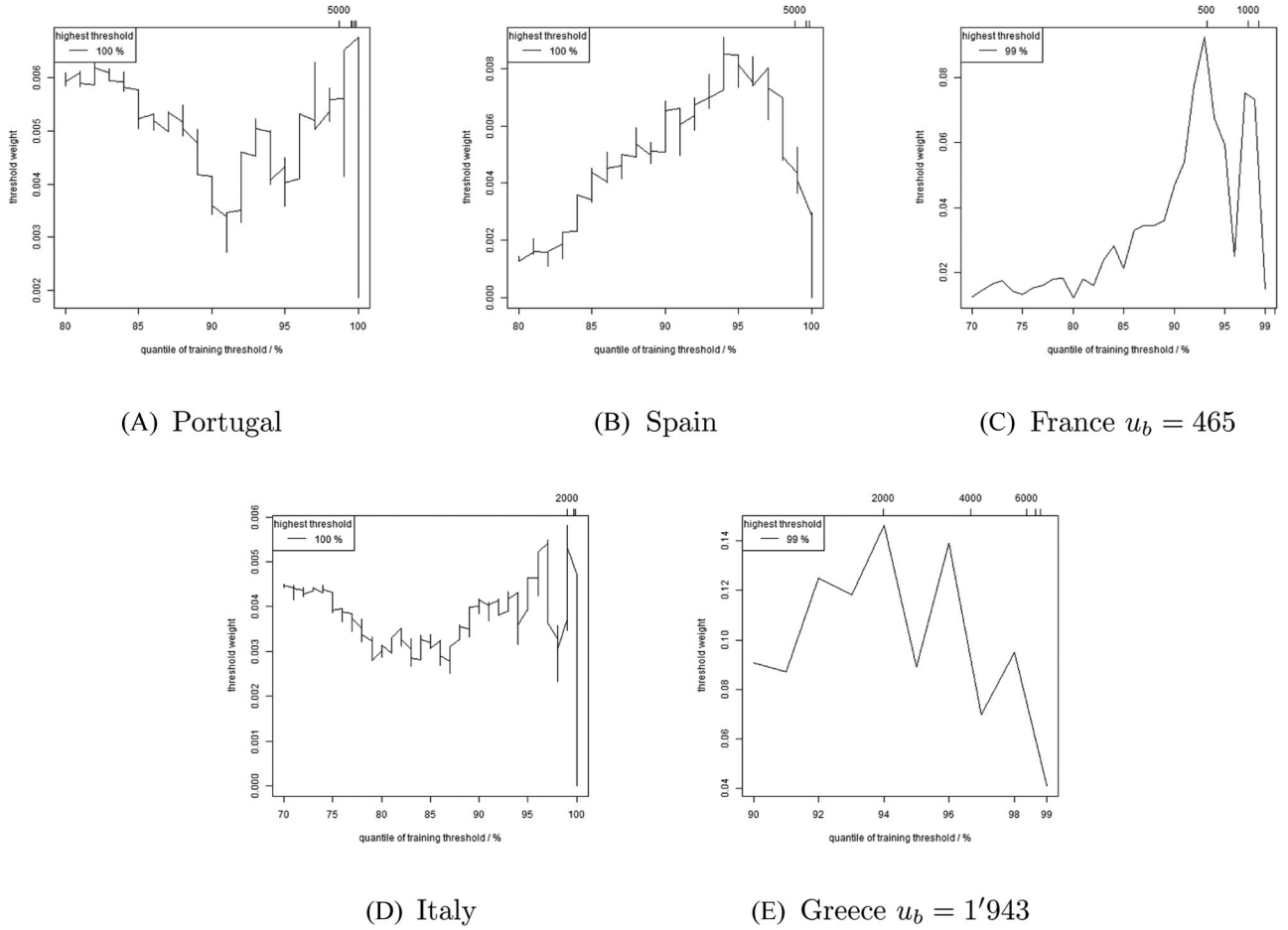

(A) Portugal (B) Spain (C) France $u_b = 465$

(D) Italy (E) Greece $u_b = 1'943$

FIGURE 4 Bayesian leave-one-out cross-validation threshold selection approach

TABLE 3 Summary statistics thresholds and extremal indices

Country	Threshold u	Extremal index θ	$n > u$ (% of total)
Portugal	4'900 ha	0.9	42 (1.4)
Spain	2'600 ha	1	62 (2.6)
France	520 ha	0.84	42 (6.3)
Italy	1'550 ha	0.94	45 (1.4)
Greece	1'943 ha	1	45 (6)

declustering.[11] The number of observations above the respective country-specific thresholds ranges from 42 to 62 and corresponds to 1.4%–6.3% of the total country-level data.

4.3 | Nonstationarity

Since the stationary models are embedded in potential nonstationary models, the results of the latter are reported first. Table 4 lists all the models with an improvement of the BIC > 10 over the stationary model following Neath and Cavanaugh (2012), suggesting this threshold as "very strong" evidence to favor the model with the lower BIC over the competing model.

For Portugal, letting the location parameter μ depend on the mean FWI for the month prior to the initial date of the fire (*FWI_MP*) leads to the best model fit. The evaluation of conditional effects for the historical excesses in Spain and Italy shows that modeling the location and the shape parameter dependent on the FWI on the reported initial date (*FWI_InitDat*) improves the model fit the most. None of the nonstationary models leads to any improvements of the model fit for Greece. For France, land cover type is found to be most influential in modeling the observed data. More specifically, modeling the location parameter conditional on land cover *Type_I* (Sclerophyllous vegetation) in a linear functional form not only proves to capture the empirical data best, but also leads to a significant positive shift of the distributional mean. However, even though modeling nonstationarity leads to an increased model fit in specific cases, with the exception of France, results do not indicate a significant modification of the modeled GEV parameters. Consequently, based on the covariates considered, the assumption of stationarity holds true in the data sample for all countries except for France. Therefore, reported probabilities of the stationary model are valid and comparable for Portugal, Spain, Italy, and Greece.

[11] The specific case of modeling the extremes with the data available for France is addressed in Section 4.3 and Section 4.4.

TABLE 4 Nonstationary models with a BIC decrease > 10 sorted by decreasing AIC

Country	Modeled parameter(s)	Modeled covariate(s)	Functional form	AIC/BIC improvement	Parameter significance
Portugal	μ	*FWI_WP*	Linear	−21.4/−19.7	μ_0 insig., $\mu_1 > 0$ *
	μ	*FWI_MP*	Quadratic	−16.2/−12.7	$\mu_0 > 0$, μ_1 insig., μ_2 insig.
Spain	μ, σ, ξ	*FWI_InitDat*	μ, ξ quadratic, σ linear	−40.0/−29.7	$\mu_0 > 0$, $\mu_1 < 0$, $\mu_2 > 0$, $\sigma_0 > 0$, σ_1 insig., ξ_0 insig., $\xi_1 > 0$, $\xi_2 < 0$ *
	μ, ξ	*FWI_InitDat*	Quadratic	−38.5/−30.3	$\mu_0 > 0$, $\mu_1 < 0$, $\mu_2 > 0$, ξ_0 insig., $\xi_1 > 0$, $\xi_2 < 0$ *
	μ	*FWI_InitDat*	Quadratic	−28.6/−24.5	μ_0 insig., μ_1 insig., μ_2 insig.
	ξ	*FWI_InitDat*	Quadratic	−24.6/−20.5	ξ_0 insig., $\xi_1 > 0$, $\xi_2 < 0$
France	μ	*Type_I*	Linear	−12.6/−11.3	$\mu_0 > 0$, $\mu_1 > 0$
Italy	μ, ξ	μ *FWI_InitDat*, ξ *FWI_InitDat/DJF*	μ quadratic, ξ interaction	−41.2/−32.3	$\mu_0 > 0$, μ_1 insig., μ_2 insig., ξ_0 insig., ξ_1 insig., $\xi_2 < 0$, ξ_3 insig. *
	μ, ξ	*FWI_InitDat*	Quadratic	−36.4/−29.3	$\mu_0 > 0$, μ_1 insig., μ_2 insig., ξ_0 insig., ξ_1 insig., ξ_2 insig. *
	μ	*FWI_InitDat*	Quadratic	−26.5/−22.9	μ_0 insig., μ_1 insig., μ_2 insig.
Greece	No model improvements				

Note: (i) Whenever the functional form is indicated as "quadratic," the linear term is included as well. (ii) In cases where the parameter 95% CIs could not be estimated via the delta method, 500 iterative bootstraps with replacement were applied to evaluate the parameter significance (indicated with *).

4.4 | Model selection/model fit

In light of no significant parameter changes modeling the extremes conditional on the implemented covariates for Portugal, Spain, Italy, and Greece, we base the subsequent model evaluations and estimations on the stationary model. Not only does the distribution of the historical extremes for France show dependence and therefore violate the stationarity assumption, but the extremal index θ in Table 2 also indicates higher dependence of the excesses than is the case for the other countries. Thus, we exclude France from subsequent analysis.

Evaluating the model fit using *Z*-plots depicted in Figure 5, it is evident that all observations lie well within the 95% confidence bands and that there is arguably a good model fit for Portugal, Spain, and Italy, and a moderately good fit for Greece. A similar conclusion can be drawn from Figure 6 plotting the kernel density functions of the empirical against the modeled data. Once again, the observed data are very well modeled for Italy, and fairly well for Portugal and Spain. For Greece, the modeled data, in contrast, captures the empirical data relatively less well.

4.5 | Parameter estimates

The three GEV distribution parameter estimates by country are shown in Table 5. The largest point estimate $\hat{\mu}$ is found for Portugal, followed by Spain, Greece, and Italy, respectively. Although the center of the distribution is larger for Spain than for Greece, $\hat{\sigma}$ indicates that the spread of the distribution is wider for Greece than for Spain. In general, we observe extremely small CIs for Portugal for the location and scale parameters.

The largest shape parameter value $\hat{\xi}$, and thus the heaviest tail, is estimated for Greece followed by Portugal and is larger than 0.5 indicating that although the mean is finite, the variance is infinite (Katz et al., 2005).[12] The point estimates of the shape parameter for Spain and Italy are fairly similar. However, $\hat{\xi}$ is insignificant for Italy. On that account, the main difference in the distributions of the extremes comparing the individual countries is that Portugal, Greece, and Spain have a significantly positive shape parameter ξ indicating a Fréchet-type limit distribution, while the excesses for Italy follow the Gumbel-type limit distribution.

4.6 | Return levels and probabilities of exceedance

Table 6 displays the numerical estimates of the *T*-year (here with $T = 5, 10, 20, 50$) BA return levels, where the BA values given in ha are exceeded in 1 year with probability $1/T$. The return levels are found to be highest in Portugal in any

[12] A statistical moment is infinite if it converges too slowly to be integrated, and thus does not exist (Holmes et al., 2008).

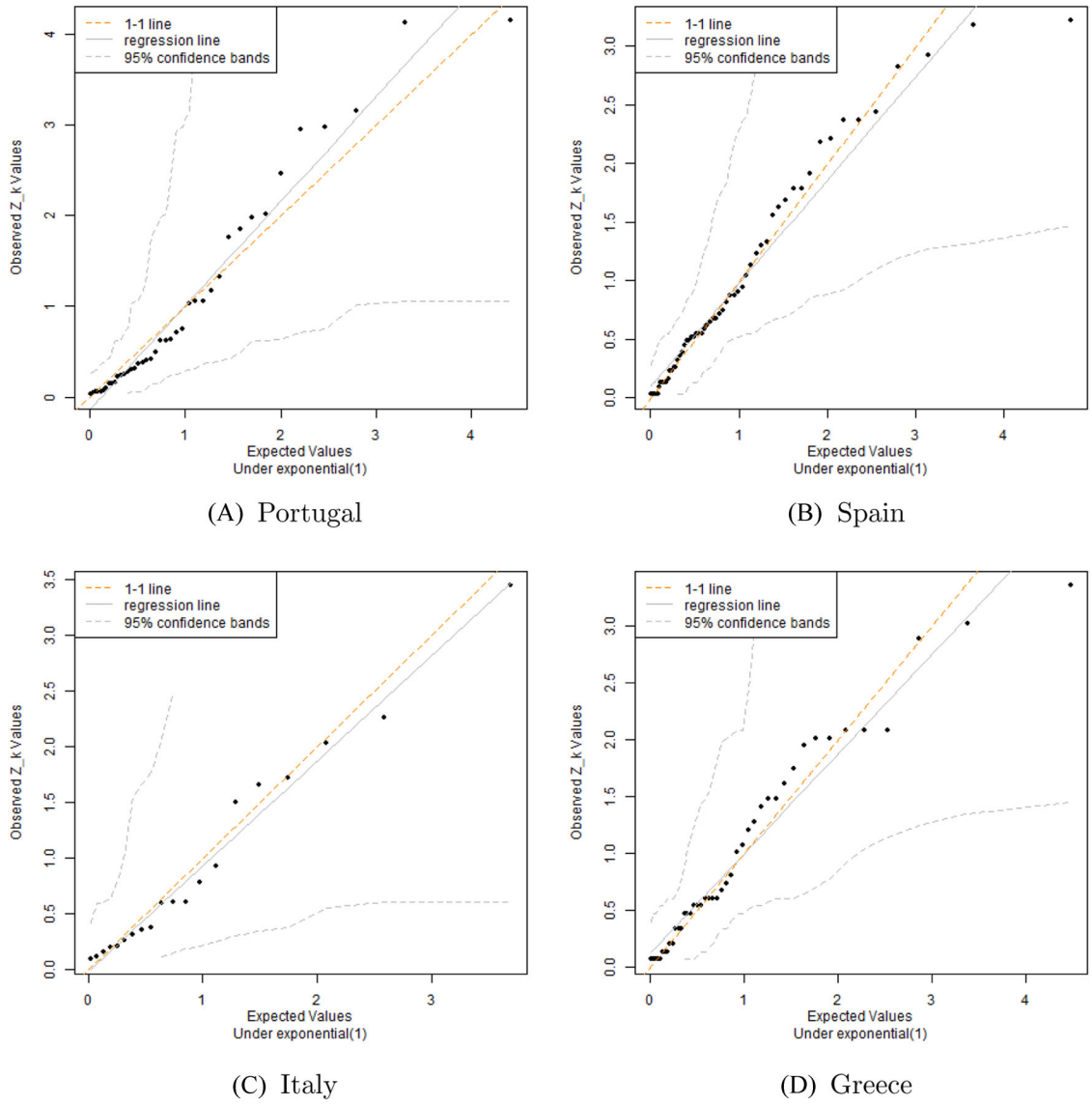

FIGURE 5 Model fit diagnostics: *Z*-plots

TABLE 5 Country-level maximum likelihood GEV parameter estimates with confidence intervals (CIs) on the 95% level

Country	Location $\hat{\mu}$ (ha)	Scale $\hat{\sigma}$ (ha)	Shape $\hat{\xi}$	Limit distribution
Portugal	13'017 (13'017, 13'017)	9'061 (9'061, 9'061)	0.52 (0.28, 0.64)	Fréchet
Spain	8'673 (8'518, 8'690)	4'719 (4'700, 4'934)	0.36 (0.28, 0.46)	Fréchet
Italy	3'483 (3'397, 3'649)	1'874 (1'539, 2'031)	0.37 (−0.06, 0.55)	Gumbel
Greece	7'206 (7'084, 7'106)	5'743 (5'742, 5'767)	0.58 (0.38, 0.69)	Fréchet

Note: The CIs are estimated employing a parametric bootstrap simulating data from the fitted model.

TABLE 6 Individual country return levels in ha for specific return periods

Country	5-year (CI)	10-year (CI)	20-year (CI)	50-year (CI)
Portugal	33'279 (30'062, 35'832)	50'338 (39'924, 58'557)	75'256 (53'038, 94'587)	123'719 (73'838, 172'805)
Spain	18'080 (17'376, 18'822)	25'165 (23'391, 26'905)	34'017 (30'277, 39'079)	49'452 (41'636, 61'197)
Italy	7'325 (6'149, 9'025)	8'966 (6'531, 12'842)	10'890 (6'944, 12'842)	14'627 (7'053, 26'704)
Greece	20'687 (18'370, 22'372)	33'242 (28'298, 37'876)	51'764 (39'636, 64'261)	91'037 (58'694, 124'476)

Note: The return levels and CIs on the 95% level are estimated employing a parametric bootstrap simulating data from the fitted model.

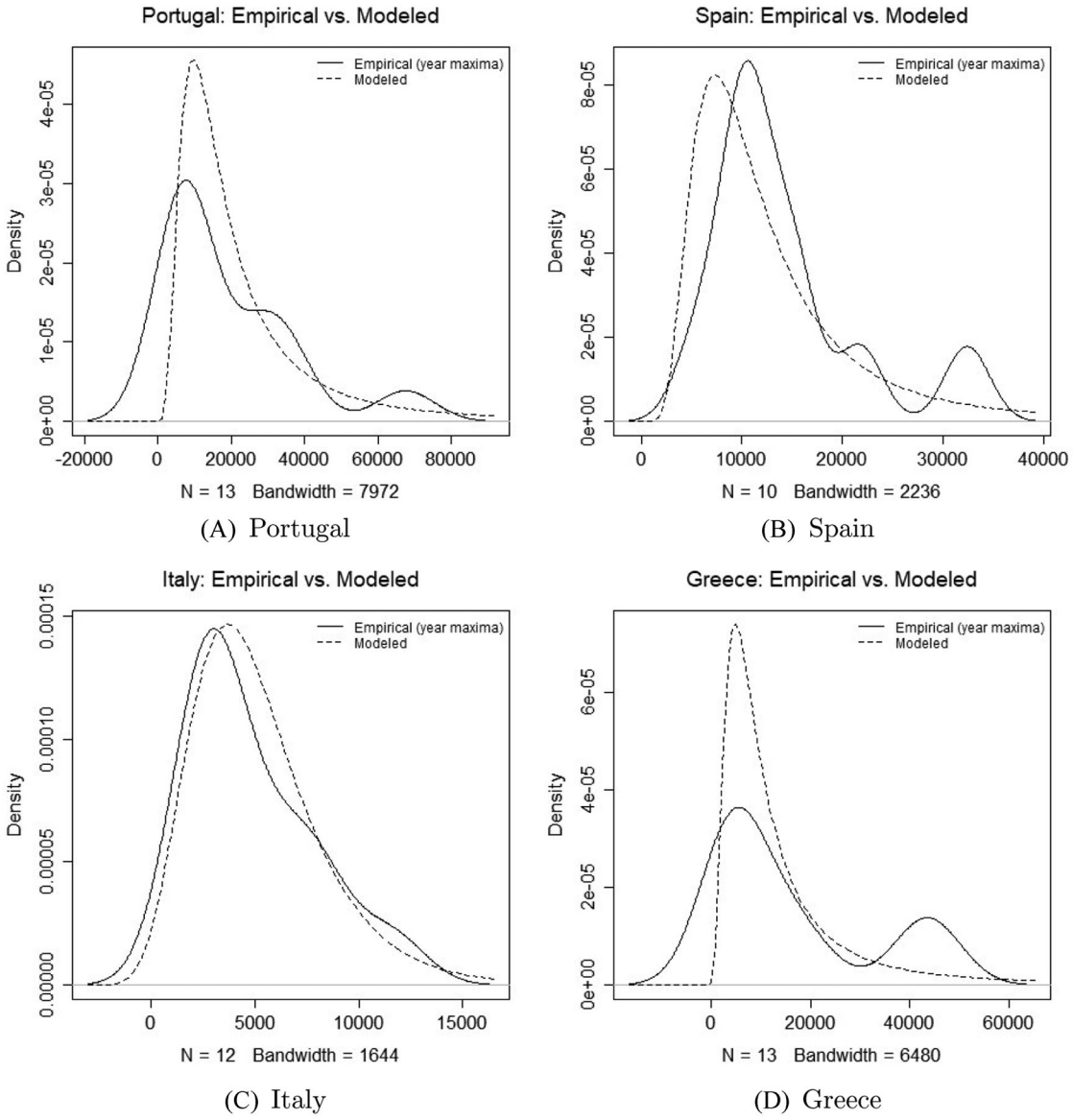

FIGURE 6 Model fit diagnostics: Density plots

given return period followed by Greece, Spain, and Italy. For example, the probability that a single wildfire burns more than 50'338 ha in any given year is 10% in Portugal, while for Spain the probability of a fire exceeding approximately this size (49'452 ha) is about 2%.

The individual country return-level plots in Figure 7 show the distribution of the observations within the tail. Essentially, the limit distributions found for all the Mediterranean countries have no upper bound (i.e., the extremes are not converging to a specific value). Furthermore, the return level plots enable a better understanding of the different limit type distributions in a graphical fashion. In particular, the distinction between the Gumbel-type distribution found for the extremes in Italy versus the Fréchet-type distributions for the other countries is distinctly visible. As the x-axis is log-transformed, the return-level plot reflects Gumbel-type distributions characterized by an exponential decay of the tail as a straight line, while the Fréchet-type distributions manifest as convex shapes.

We find that all the observed events lie within the bootstrapped CIs. Furthermore, the smallest confidence bands at the 95% level are observed for Spain indicating high certainty of the point estimates. In contrast, the largest CIs are apparent for Italy suggesting a wide range of potential outcomes within the 95% CI.

Looking at the largest wildfire for each country (max value in Table 2), an event of such size or larger is expected to occur, on average, once every 16 years for Portugal with an annual occurrence probability of 1.9%. The calculated yearly probability for the largest observed fire in Spain is 1% and has a return period of about 18 years. In Italy, the maximum BA value is expected to be exceeded once in every 23 years with an annual probability of 2.6%, and the largest BA value for Greece, is estimated as an approximately 16-year event

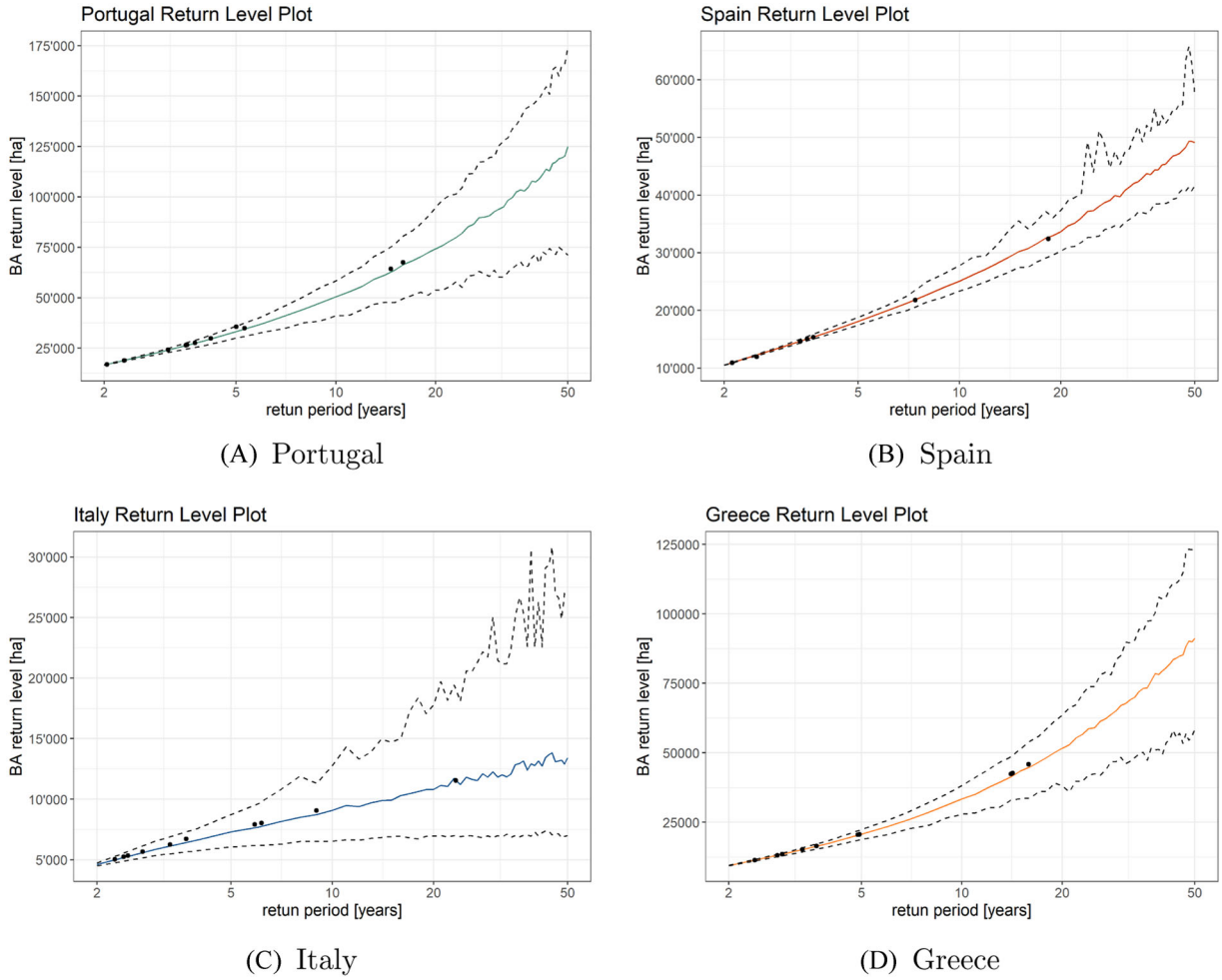

FIGURE 7 Return-level plots with bootstrapped CIs on the 95% level

with a yearly probability of occurrence of 1.8%. Figure 8 overlays the individual country return-level plots to facilitate a cross-country comparison of the extremal BA distribution. We find the highest risk for extremely large fires for any given return period for Portugal and the lowest for Italy. Comparing Greece and Spain, a higher risk for large BAs emerges for Spain for low return periods (approximately < 3 years) but above this threshold, the return levels are distinctively larger for Greece.

A similar picture emerges when overlying the individual country-level BA thresholds that are exceeded in any given year with corresponding probabilities shown in Figure 9. The annual probability for extremely large fires decreases fastest for Italy and slowest for Portugal. The rate of the yearly probability decrease is comparably close for Spain and Greece with the ξ parameter point estimates only differing marginally.

4.7 | Economic valuation

Combining our results with the economic loss figures in €/ha leads to expected return period–specific economic losses presented in Table 7. Allowing a comparison of the individual publications' loss calculations, Figure 10 graphically displays the economic loss estimates for wildfires that are expected to occur, on average once every 20 years.

TABLE 7 Range of country-level economic loss estimates for specific return levels (rl) in million € (in 2020€)

Country	5-year rl	10-year rl	20-year rl	50-year rl
Portugal	107–290	162–439	243–656	400–1'078
Spain	58–158	81–219	110–297	160–431
Italy	15–64	18–78	22–95	29–128
Greece	25–180	41–290	64–451	11–794

Recall from Table 1, that while the estimates by Butry et al. (2001), Rahn et al. (2014), and Barrio et al. (2007) are relatively close, the country-specific €/ha estimate based on the figures in Merlo and Croitoru (2005) is lower than the other three for Italy and Greece, and higher for Portugal. The latest study conducted by Safford et al. (2022) clearly stands out with a distinctively larger loss estimate value.

In addition to providing economic loss estimates for specific return periods resulting from the extreme value mod-

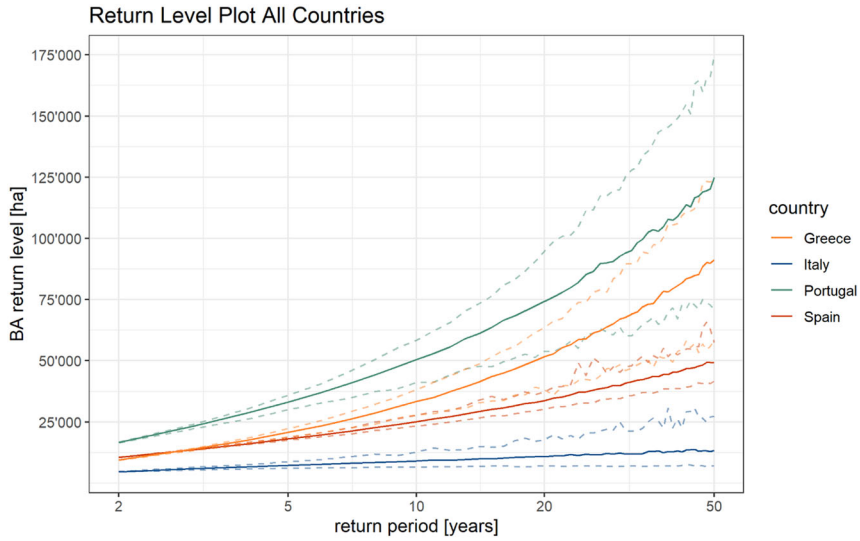

FIGURE 8 All country return-level plot

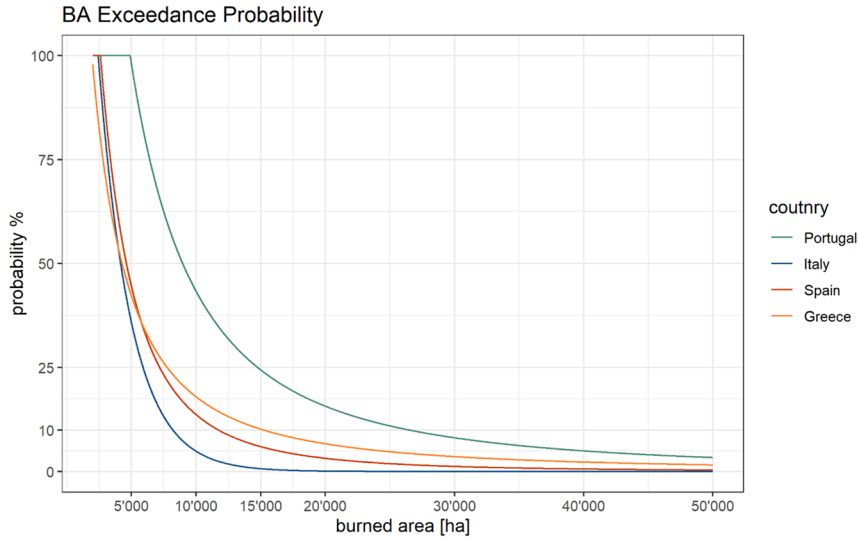

FIGURE 9 Country-level BA exceedance probabilities in any given year

eling, we also show cost estimates based on the single largest observed wildfires in the study period for each country. Hence, the cost estimates come from multiplying the maximum events in Table 2 by the corresponding €/ha estimates derived from the existing literature. The largest wildfire event leads to an economic loss estimate of 218–589 million € for Portugal, 105–283 million € for Spain, 23–101 million € for Italy, and 56–399 million € for Greece for a specific event of that magnitude.

5 | DISCUSSION

5.1 | Implications

With the quantification of country-level risk of extreme wildfires, we are able to contribute to the empirical evidence to information-based decision making regarding forest management for various stakeholders. Providing reliable estimates of return periods arguably has important implications for government agencies looking to adjust budget planning for fire prevention measures and suppression spending. Furthermore, the quantification of large fire risk through return levels can provide useful information for landowners regarding long-term investment and forest management choices, or for other institutions such as reinsurance companies. Moreover, the knowledge of the wildfire risk could also be used to increase awareness and thus may affect decision making at the individual level (i.e., location choices, property protection measures, investment in insurance associated with wildfire damage). Converting the return-level estimates of extreme wildfires in Mediterranean Europe to monetary values, as we did here, arguably provides an important tool for policy-related cost–benefit analyses. For example, the associated monetary values with a return period event can assist a government in the budget allocation of both fire prevention and suppression spending by comparing their expenditures with the expected losses

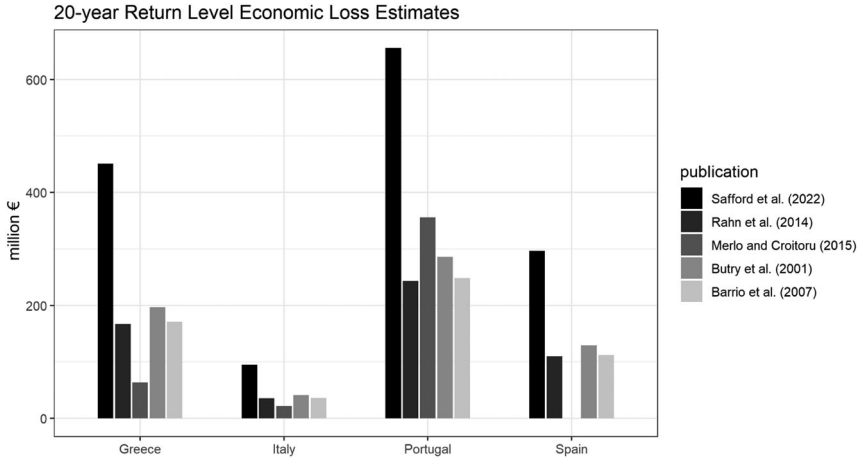

FIGURE 10 Country-level economic loss estimates for the 20-year return period

particularly for extremely large wildfires over a specific time period.

Examining the specific results, it is insightful to first reflect on the implications of the different distributions of extreme wildfires estimated for the individual countries in our analysis. Most importantly, we find that these rare events follow a Fréchet-type distribution for Portugal, Spain, and Greece. This is in line with regional estimates within Portugal by De Zea Bermudez et al. (2009) and Scotto et al. (2014). Out of the three limit-type distributions, the Fréchet distribution has the heaviest tail indicating that the probability of rare events is much higher than commonly perceived (i.e., "extreme" wildfires are not as surprising). However, although the point estimate of the shape parameter is very similar for Spain and Italy, it is not found to be significantly positive for Italy, implying that the respective extremes follow a Gumbel distribution characterized by a lighter tail than for the other Mediterranean countries. Thus, extremely large wildfires are expected to occur less often in Italy than in Spain. Overall, we find the largest point estimate of the shape parameter of 0.58 for Greece, followed by a value of 0.52 for Portugal. This indicates that the probability of extremely large wildfires is highest in Greece when only the shape parameter of the extreme event distribution is considered (i.e., excluding the mean and the spread of the distribution). Notably, both the Fréchet and the Gumbel distribution do not converge to an upper limit but are unbounded. As a matter of fact, the extremes, and thus the associated losses, characterized by the Fréchet distribution, are limitless.

The return-level results derived from the inclusion of all the three parameter estimates (location, scale, and shape) indicate the highest risk of extremely large wildfires across all evaluated return periods in Portugal and the lowest risk in Italy. Comparing Greece and Portugal, the return level for up to about 3-year events is higher in Spain, but for any return period above, it is found to be higher for Greece. For instance, the individual country return levels for 10-year return period events are 50'338 ha (PT), 33'242 ha (GR), 25'165 ha (ES), and 8'966 ha (IT). For wildfires, which are expected to occur on average once in 20 years, the return levels are estimated at 75'256 ha (PT), 51'764 ha (GR), 34'017 ha (ES), and 10'890 ha (IT).

Our data do not suggest that the FWI, which captures relative fire danger, affects the distribution of wildfire occurrence or their magnitude. Ideally, we would have a much longer time series, which would make it possible to detect climatological changes. This means our results should be interpreted with care. In this regard, it must be pointed out that while many climate change projections suggest that Southern Europe faces an increasing risk in extreme wildfires (Bowman et al., 2017; De Rigo et al., 2017; Turco et al., 2018), Batllori et al. (2013) indicate that fire activity predictions can be highly divergent particularly regarding precipitation-related variables. Notwithstanding the wildfire risk driven by future climate conditions, evidence also suggests that the risk associated with human exposure may increase especially with projected population growth in fire-prone regions (Knorr et al., 2016; Turco et al., 2019). Even though we did not find evidence supporting a time trend in our study, it is crucial to continue efforts to better understand the risk associated with wildfires for Mediterranean Europe. Going forward, more comprehensive and harmonized data are needed to evaluate future extreme wildfire risk scenarios incorporating climatic and demographic components as well as more detailed information on the individual fires (e.g., duration, severity, ignition point, cause) in order to distinguish which factors have the potential to influence the extremely large fires.

5.2 | Limitations

Although predictions of events not actually observed in the historical data are common with the use of EVT methods, we need to emphasize that our estimates are based on data for a particularly short time period of 14 years. In this regard, encounter probability[13] suggests that the probability

[13] The encounter probability $P_e = 1 - (1 - \frac{1}{T})^n$ is the likelihood of observing a T-return period event within a specific time period denoted by n.

of observing a 5-year event given our data is approximately 96%, a 10-year event 77%, a 20-year event 51%, and a 50-year event 25%, and only our 10- and 20-year event estimates are based on events witnessed in the sample period. The short time period of data may also play a role in the nonstationarity results. Although modeling the threshold excesses conditional on factors potentially influencing the distribution of extreme wildfires does lead to an improved capture of the empirical data for all countries but Greece, none of the models significantly changed the extremal distribution. Whereas it is not given that the included variables would lead to a change in the distribution of extremely large wildfires with a prolonged time period, a potential underlying dependence on factors driving or affecting extreme BA is more difficult to detect in shorter periods of analysis.

The coupling of our estimated BA return levels with existing economic loss figures also comes with strong caveats, particularly with regard to regional and temporal transfers of monetary estimates, as well as through the distinct study designs incorporating disparate economic variables in the respective loss calculations. For example, only Barrio et al. (2007) and Butry et al. (2001) include any estimation of wildfire-related health costs, which are of significant magnitude and thus, of rising concern as pointed out in Black et al. (2017). Furthermore, even though Merlo and Croitoru (2005) address country-level estimates of indirect use, option, bequest, and existence values of forests in general, they are not applied to the BA scenario and only the estimate provided by Safford et al. (2022) includes ecological (vegetation and wildlife) damage. Moreover, as the monetary valuation of indirect costs poses great challenges, besides the impediment imposed by oftentimes limited data availability particularly driven by methodological restraints, many loss calculations focus on direct impacts. However, the indirect costs are likely to exceed the reported costs as argued in CCST (2020). Thus, our calculations are conservative and the considered losses are likely to represent only some fraction of the actual economic impact. Nevertheless, our results still provide some indication of the serious implications wildfires have for many other sectors that they can reach far beyond the commonly assessed impacts.

In terms of examining the role of covariates in potential changes in the distribution of extreme wildfires, the FWI may not be the most suitable variable to capture those. Jiménez-Ruano et al. (2019) conclude that although the FWI provides useful information regarding seasonal variability and near-future trends, it is not necessarily the most advisable index to detect long-term trends. In this regard however, Pérez-Sánchez et al. (2017) do identify the FWI as the most suitable index for fire-risk ignition and spreading in semiarid areas such as the Iberian Peninsula. Likewise, De Rigo et al. (2017) point out that the FWI is well suited as a harmonized index over different regions for weather-driven fire danger, and Fernandes et al. (2016) observe that particularly large fires exhibit stronger responses to the severity of the fire weather.

With respect to the population density covariate, Bowman et al. (2017) demonstrate that large destructive wildfires are most likely to occur in a two-sided bounded area that excludes either very sparsely or densely populated areas, and thus highlights the underlying complexity of this interdependence. On this account, our study design calculating the mean population density around the center of a BA, might arguably be an unsatisfactory way to capture this intricate relationship, given there exists one for the extremely large fires in the studied geographical area. Additionally, we do see that many of the population density values for the extreme wildfires in our data set lie within a narrow range leading to small explanatory power of the variable. Having information on the exact ignition location of a fire might contribute to the evaluation of the potential association between population density and extreme wildfire occurrence.

Regarding the land cover type, we face a slightly different problem as it is implemented as a categorical variable. As we look at the extremes, we focus on solely on 42–62 observations for each country, and thus, we need to strictly limit the number of categories to forego having only very few wildfires for each of those. Therefore, we categorize the extreme wildfires into four main country-specific land cover–type classes, and thereby sacrifice some of the specificity. Comparable drawbacks arise from the categorical covariates capturing seasonality as the extremely large wildfires are assigned to one of the four seasons. However, in this case, it is less a problem of simplification but rather one of unequally distributed observations per category, particularly as "off-wildfire season" categories arguably contain very few observations.

For the specific case of France, we note that compared to the other countries the data are more challenging to work with. Although it is typical for all the Mediterranean countries that certain years stand out with more severe fire seasons, this is particularly pronounced for the wildfire records in France with more than half of the observations coming from 2019. This in turn leads to a comparably high dependence of the extreme observations as many of the largest wildfires are recorded in a single year. Furthermore, in contrast to the other European Mediterranean countries, France geographically expands much further North, and is thus characterized by more diverse land cover types. Hence, the finding that a specific land cover type, namely, Sclerophyllous vegetation, leads to a positive shift in the distribution of the extremes might indicate that this is the vegetation type most dominant at the Mediterranean coastline and may be correlated with extreme wildfires.[14]

6 | CONCLUSION

In this article, we assemble a high-quality homogeneous up-to-date geospatial data set for Mediterranean Europe and

[14] Although the aim of this article is to model and compare country-level data, future research may benefit from regional modeling, which may be particularly useful for the case of France where there is considerable heterogeneity in wildfire occurrence primarily between the North and the South of the country (and Corsica).

perform a cross-country risk analysis of extreme wildfires defined by BA. Although modeling a variety of covariates with the potential to affect the extremal distributions, we find no evidence for nonstationarity in the observed study period. Furthermore, the threshold excesses for France in the data set do not fulfill underlying assumptions to carry out a sound EVT analysis, and are thus only included in the descriptive part. In our results, we find the highest risk for extremely large wildfires in Portugal, followed by Greece, Spain, and Italy. We estimate the return levels for 5-, 10-, 20-, and 50-year return period events and combine our outcomes with the existing literature on economic costs. The robust estimation of extreme wildfire events underlying an evidence-based risk assessment is arguably beneficial for governmental bodies, reinsurance institutions, landowners, and residents in wildfire-prone areas providing support in information-based decision-making processes.

We emphasize the need to build international homogeneous comprehensive databases with high spatial and temporal resolution regarding wildfire occurrence (ideally including point of origin, duration, and cause) but also dedicated to associated measures such as prevention and suppression spending, as well as individual fire event impact on ecosystems, infrastructures, properties, and people. Accompanying the extensive WUI with exposed communities particularly at the highly populated coastal areas of Southern Europe and vulnerable ecosystems across the region, extreme wildfire events continue to pose a substantial environmental hazard for Mediterranean Europe in the future.

ACKNOWLEDGMENT

This project has received funding from the European Union's Horizon 2020 research and innovation program under the Marie Skłodowska-Curie Grant Agreement Innovative Training Networks (ITN) No. 860787.

ORCID

Sarah Meier https://orcid.org/0000-0001-6108-0735
Robert J. R. Elliott https://orcid.org/0000-0002-3966-2082
Nicholas Kettridge https://orcid.org/0000-0003-3995-0305

REFERENCES

Barrio, M., Loureiro, M., & Chas, M. L. (2007). Aproximación a las pérdidas económicas ocasionadas a corto plazo por los incendios forestales en Galicia en 2006. *Economía Agraria y Recursos Naturales*, *7*(14), 45–64.

Batllori, E., Parisien, M. A., Krawchuk, M. A., & Moritz, M. A. (2013). Climate change-induced shifts in fire for Mediterranean ecosystems. *Global Ecology and Biogeography*, *22*(10), 1118–1129.

Bedia, J., Herrera, S., Camia, A., Moreno, J. M., & Gutiérrez, J. M. (2014). Forest fire danger projections in the Mediterranean using ENSEMBLES regional climate change scenarios. *Climatic Change*, *122*(1-2), 185–199.

Beverly, J. L., & Martell, D. L. (2005). Characterizing extreme fire and weather events in the Boreal Shield ecozone of Ontario. *Agricultural and Forest Meteorology*, *133*(1-4), 5–16.

Black, C., Tesfaigzi, Y., Bassein, J. A., & Miller, L. A. (2017). Wildfire smoke exposure and human health: Significant gaps in research for a growing public health issue. *Environmental Toxicology and Pharmacology*, *55*, 186–195.

Bowman, D. M., Williamson, G. J., Abatzoglou, J. T., Kolden, C. A., Cochrane, M. A., & Smith, A. M. (2017). Human exposure and sensitivity to globally extreme wildfire events. *Nature Ecology and Evolution*, *1*(3), 1–6.

Butry, D. T., Mercer, D. E., Prestemon, J. P., Pye, J. M., & Holmes, T. P. (2001). What is the price of catastrophic wildfire? *Journal of Forestry*, *99*(11), 9–17.

Camia, A., Amatulli, G., & San-Miguel-Ayanz, J. (2008). Past and future trends of forest fire danger in Europe. Technical report, Joint Research Centre.

CCST (2020). *The costs of wildfire in California: An independent review of scientific and technical information*. Technical report, California Council on Science and Technology, Sacramento, California.

Coles, S. (2001). *An introduction to statistical modeling of extreme values*. Springer.

De Rigo, D., Libertà, G., Houston Durrant, T., Artés Vivancos, T., & San-Miguel-Ayanz, J. (2017). *Forest fire danger extremes in Europe under climate change: Variability and uncertainty*. Technical report, Publication Office of the European Union, Luxembourg.

De Zea Bermudez, P., Mendes, J., Pereira, J. M., Turkman, K. F., & Vasconcelos, M. J. (2009). Spatial and temporal extremes of wildfire sizes in Portugal. *International Journal of Wildland Fire*, *18*(8), 983–991.

Evin, G., Curt, T., & Eckert, N. (2018). Has fire policy decreased the return period of the largest wildfire events in France? A Bayesian assessment based on extreme value theory. *Natural Hazards and Earth System Sciences*, *18*(10), 2641–2651.

Fernandes, P. M. (2019). Variation in the canadian fire weather index thresholds for increasingly larger fires in Portugal. *Forests*, 838 (Online version).

Fernandes, P. M., Barros, A. M., Pinto, A., & Santos, J. A. (2016). Characteristics and controls of extremely large wildfires in the western Mediterranean Basin. *Journal of Geophysical Research: Biogeosciences*, *121*(8), 2141–2157.

Ferro, C. A., & Segers, J. (2003). Inference for clusters of extreme values. *Royal Statistical Society*, *65*(2), 545–556.

Gill, A. M., & Allan, G. (2008). Large fires, fire effects and the fire-regime concept. *International Journal of Wildland Fire*, *17*(6), 688–695.

Gilleland, E., & Katz, R. W. (2016). ExtRemes 2.0: An extreme value analysis package in R. *Journal of Statistical Software*, *72*(8), 1–39.

González-Cabán, A. (2009). *Proceedings of the third international symposium on fire economics, planning, and policy: Common problems and approaches*. Technical report, United States Department of Agriculture, Forest Service, Albany, California.

Hernandez, C., Keribin, C., Drobinski, P., & Turquety, S. (2015). Statistical modelling of wildfire size and intensity: A step toward meteorological forecasting of summer extreme fire risk. *Annales Geophysicae*, *33*(12), 1495–1506.

Holmes, T. P., Prestemon, J. P., & Abt, K. L. (2008). *An introduction to the economics of forest disturbance*. Springer.

Jiang, Y., & Zhuang, Q. (2011). Extreme value analysis of wildfires in Canadian boreal forest ecosystems. *Canadian Journal of Forest Research*, *41*(9), 1836–1851.

Jiménez-Ruano, A., Rodrigues Mimbrero, M., Jolly, W. M., & de la Riva Fernández, J. (2019). The role of short-term weather conditions in temporal dynamics of fire regime features in Mainland Spain. *Journal of Environmental Management*, *241*, 575–586.

Katz, R. W., Brush, G. S., & Parlange, M. B. (2005). Statistics of extremes: Modeling ecological disturbances. *Ecology*, *86*(5), 1124–1134.

Keeley, J. E., Bond, W. J., Bradstock, R. A., Pausas, J. G., & Rundel, P. W. (2012). *Fire in Mediterranean ecosystems: Ecology, evolution and management*. Cambridge University Press.

Keyser, A. R., & Westerling, A. L. R. (2019). Predicting increasing high severity area burned for three forested regions in the western United States using extreme value theory. *Forest Ecology and Management*, *432*, 694–706.

Knorr, W., Arneth, A., & Jiang, L. (2016). Demographic controls of future global fire risk. *Nature Climate Change*, *6*(8), 781–785.

Krawchuk, M. A., Cumming, S. G., & Flannigan, M. D. (2009). Predicted changes in fire weather suggest increases in lightning fire initiation and future area burned in the mixedwood boreal forest. *Climatic Change*, *92*(1-2), 83–97.

Lankoande, M., & Yoder, J. (2006). *An econometric model of wildfire suppression productivity*. Washington State University School of Economic Sciences, 1–23.

McElhinny, M., Beckers, J. F., Hanes, C., Flannigan, M., & Jain, P. (2020). A high-resolution reanalysis of global fire weather from 1979 to 2018—Overwintering the drought code. *Earth System Science Data*, *12*(3), 1823–1833.

Mendes, J. M., de Zea Bermudez, P. C., Pereira, J., Turkman, K. F., & Vasconcelos, M. J. (2010). Spatial extremes of wildfire sizes: Bayesian hierarchical models for extremes. *Environmental and Ecological Statistics*, *17*(1), 1–28.

Merlo, M., & Croitoru, L. (2005). *Valuing Mediterranean forests—Towards total economic value*. CABI Publishing.

Myers, N., Mittermeier, R. A., Mittermeier, C. G., da Fonseca, G. A. B., & Kent, J. (2000). Biodiversity hotspots for conservation priorities. *Nature*, *403*, 853–858.

NATURE (2017). Spreading like wildfire. *Nature Climate Change*, *7*(11), 755, https://www.nature.com/articles/nclimate3432

Neath, A. A., & Cavanaugh, J. E. (2012). The Bayesian information criterion: Background, derivation, and applications. *Wiley Interdisciplinary Reviews: Computational Statistics*, *4*(2), 199–203.

Northrop, P. J., & Attalides, N. (2020). *threshr: Threshold selection and uncertainty for extreme value analysis*. R package version 1.0.3, https://CRAN.R-project.org/package=threshr

Northrop, P. J., Attalides, N., & Jonathan, P. (2017). Cross-validatory extreme value threshold selection and uncertainty with application to ocean storm severity. *Journal of the Royal Statistical Society*, *66*(1), 93–120.

Pechony, O., & Shindell, D. T. (2010). Driving forces of global wildfires over the past millennium and the forthcoming century. *Proceedings of the National Academy of Sciences of the United States of America*, *107*(45), 19167–19170.

Pérez-Sánchez, J., Senent-Aparicio, J., Díaz-Palmero, J. M., & Cabezas-Cerezo, J. d. D. (2017). A comparative study of fire weather indices in a semiarid south-eastern Europe region. Case of study: Murcia (Spain). *Science of the Total Environment*, *590-591*, 761–774.

Pickands, J. (1971). The two-dimensional poisson process and extremal processes. *Journal of Applied Probability*, *8*(4), 745–756.

Rahn, M., Hale, K., Brown, C., & Edwards, T. (2014). *Economic impacts of wildfires: 2003 San Diego wildfires in retrospect*. Technical report, San Diego State University Wildfire Research Center.

Safford, H. D., Paulson, A. K., Steel, Z. L., Young, D. J., & Wayman, R. B. (2022). The 2020 California fire season: A year like no other, a return to the past or a harbinger of the future? *Global Ecology and Biogeography*, 1–21.

San-Miguel-Ayanz, J., Durrant, T., Boca, R., Liberta, G., Branco, A., de Rigo, D., Ferrari, D., Maianti, P., Vivancos, T. A., Costa, H., Lana, F., Löffler, P., Nuijten, D., Anders, C. A., & Thais, L. (2018). *Forest fires in Europe, Middle East and North Africa 2017*. Technical report, Joint Research Centre.

San-Miguel-Ayanz, J., Durrant, T., Boca, R., Malanti, P., Libertà, G., Artés-Vivancos, T., Oom, D., Branco, A., de Rigo, D., Ferrari, D., Pfeiffer, H., Grecchi, R., Nuijten, D., & Leray, T. (2020). *Forest fires in Europe, Middle East and North Africa 2019*. Technical report, Joint Research Center, Luxembourg.

San-Miguel-Ayanz, J., Moreno, J. M., & Camia, A. (2013). Analysis of large fires in European Mediterranean landscapes: Lessons learned and perspectives. *Forest Ecology and Management*, *294*, 11–22.

Santín, C., & Doerr, S. H. (2016). Fire effects on soils: The human dimension. *Philosophical Transactions of the Royal Society B: Biological Sciences*, *371*(1696), 28–34.

Scotto, M. G., Gouveia, S., Carvalho, A., Monteiro, A., Martins, V., Flannigan, M. D., San-Miguel-Ayanz, J., Miranda, A. I., & Borrego, C. (2014). Area burned in Portugal over recent decades: An extreme value analysis. *International Journal of Wildland Fire*, *23*(6), 812–824.

Smith, R. L. (1989). Extreme value analysis of environmental time series: An application to trend detection in ground-level ozone. *Statistical Science*, *4*(4), 367–377.

Smith, R. L., & Shively, T. S. (1995). Point process approach to modeling trends in tropospheric ozone based on exceedances of a high threshold. *Atmospheric Environment*, *29*(23), 3489–3499.

Sousa, P. M., Trigo, R. M., Pereira, M. G., Bedia, J., & Gutiérrez, J. M. (2015). Different approaches to model future burnt area in the Iberian Peninsula. *Agricultural and Forest Meteorology*, *202*, 11–25.

Tedim, F., Leone, V., Amraoui, M., Bouillon, C., Coughlan, M., Delogu, G., Fernandes, P., Ferreira, C., McCaffrey, S., McGee, T., Parente, J., Paton, D., Pereira, M., Ribeiro, L., Viegas, D., & Xanthopoulos, G. (2018). Defining extreme wildfire events: Difficulties, challenges, and impacts. *Fire*, *1*(1), 9.

Turco, M., Herrera, S., Tourigny, E., Chuvieco, E., & Provenzale, A. (2019). A comparison of remotely-sensed and inventory datasets for burned area in Mediterranean Europe. *International Journal of Applied Earth Observation and Geoinformation*. 101887 (Online version).

Turco, M., Rosa-Cánovas, J. J., Bedia, J., Jerez, S., Montávez, J. P., Llasat, M. C., & Provenzale, A. (2018). Exacerbated fires in Mediterranean Europe due to anthropogenic warming projected with non-stationary climate-fire models. *Nature Communications*, *9*(1), 1–9.

Van Wagner, C. E., & Pickett, T. L. (1985). *Equations and FORTRAN program for the canadian forest fire weather index system*. Technical report, Canadian Forestry Service, Ottawa.

Wang, D., Guan, D., Zhu, S., Kinnon, M. M., Geng, G., Zhang, Q., Zheng, H., Lei, T., Shao, S., Gong, P., & Davis, S. J. (2021). Economic footprint of California wildfires in 2018. *Nature Sustainability*, *4*(3), 252–260.

SUPPORTING INFORMATION

Additional supporting information can be found online in the Supporting Information section at the end of this article.

How to cite this article: Meier, S., Strobl, E., Elliott, R. R., & Kettridge, N. (2022). Cross-country risk quantification of extreme wildfires in Mediterranean Europe. *Risk Analysis*, 1–18. https://doi.org/10.1111/risa.14075

Journal of Environmental Economics and Management 118 (2023) 102787

Contents lists available at ScienceDirect

Journal of Environmental Economics and Management

journal homepage: www.elsevier.com/locate/jeem

The regional economic impact of wildfires: Evidence from Southern Europe☆

Sarah Meier [a,*], Robert J.R. Elliott [b], Eric Strobl [c]

[a] School of Geography, Earth and Environmental Sciences, University of Birmingham, Edgbaston, Birmingham B15 2TT, United Kingdom
[b] Department of Economics, University of Birmingham, United Kingdom
[c] Department of Economics, University of Bern, Switzerland

ARTICLE INFO

JEL classification:
O4
Q5
R1

Keywords:
GDP growth
Employment growth
Natural disasters
Wildfire

ABSTRACT

We estimate the impact of wildfires on the growth rate of gross domestic product (GDP) and employment of regional economies in Southern Europe from 2011 to 2018. To this end we match Eurostat economic data with geospatial burned area perimeters based on satellite imagery for 233 Nomenclature of Territorial Units for Statistics (NUTS) 3 level regions in Portugal, Spain, Italy, and Greece. Our panel fixed effects instrumental variable estimation results suggest an average contemporary decrease in a region's annual GDP growth rate of 0.11–0.18% conditional on having experienced at least one wildfire. For an average wildfire season this leads to a yearly production loss of 13–21 billion euros for Southern Europe. The impact on the employment growth rate is heterogeneous across economic activity types in that there is a decrease in the average annual employment growth rate for activities related to retail and tourism (e.g., transport, accommodation, food service activities) of 0.09–0.15%, offset by employment growth in insurance, real estate, administrative, and support service related activities of 0.13–0.22%.

1. Introduction

In recent years news coverage of orange coloured skies, evacuations, and devastation caused by wildfires has become all too familiar. Even though one tends to only hear about the most calamitous and tragic of fires, every summer Southern European countries experience a large number of fires of varying degrees of seriousness (San-Miguel-Ayanz et al., 2021, 2022). These events can be highly disruptive and destructive, affecting different sectors of the economy, such as forestry and agriculture (Butry et al., 2001; Rego et al., 2013), industry and construction (Kramer et al., 2021; Wang et al., 2021), and recreation and tourism (Kim and Jakus, 2019; Molina et al., 2019; Gellman et al., 2022; Otrachshenko and Nunes, 2022). Importantly, natural disasters, including wildfires, are for the most part localised events that are likely to induce predominantly local effects that could potentially be disguised if one only considers aggregated data at the national level (Horwich, 2000).[1] Given increasing European regional inequality particularly in Southern Europe (Iammarino et al., 2019) and the possibility that the region faces an increased risk of wildfires due to climate change (Dupuy et al., 2020; Sullivan et al., 2022), being able to identify and quantify the potential economic impact of

☆ This work was supported by the European Union's Horizon 2020 research and innovation program under the Marie Skłodowska-Curie grant agreement Innovative Training Networks No. 860787. Any results, opinions and conclusions expressed in this work are those of the authors and do not necessarily reflect the views of the funding organisation.

* Corresponding author.
E-mail addresses: s.meier@bham.ac.uk (S. Meier), r.j.elliott@bham.ac.uk (R.J.R. Elliott), eric.strobl@vwi.unibe.ch (E. Strobl).

[1] Wildfires may also have more wide reaching effects through drifting smoke pollution although this aspect is not specifically considered in this study.

https://doi.org/10.1016/j.jeem.2023.102787
Received 2 May 2022
Available online 21 January 2023

wildfires has important implications for regional policy making. In this paper we explicitly set out to examine the regional gross domestic product (GDP) and employment impacts of wildfires in Southern Europe since 2010.

There is now a sizeable theoretical and empirical literature focusing on the impacts of natural disasters other than wildfires on GDP growth. For example, negative effects are found after hurricanes (Strobl, 2011), cyclones (Naguib et al., 2022), and floods (Parida et al., 2021). Furthermore, Barone and Mocetti (2014) show a short-term negative effect on GDP growth from a study of two earthquakes in Italy, but report a positive long-term effect for one of them. While a majority of studies do report predominantly negative effects, the literature does not offer conclusive evidence and impacts depend on a variety of dimensions, such as on severity, disaster type, and country of occurrence (Loayza et al., 2012; Fomby et al., 2013). Nevertheless, conducting a meta-analysis using more than 750 estimates from publications studying the relationship between natural disasters, Klomp and Valckx (2014) conclude that there is a genuine negative effect that is increasing over time. Similarly, Felbermayr and Gröschl (2014) construct a comprehensive disaster data set from geophysical and meteorological information as opposed to using insurance data, and also find a robust negative effect of natural disasters on GDP growth.

A number of studies have also examined the employment impact of natural disasters, although the evidence is scarcer and much more mixed. As Deryugina (2022) notes, natural disasters can affect the labour market equilibrium through a number of different channels. For example, if areas that heavily rely on tourism are impacted, employment in the hospitality sector is likely to fall. For example, Barattieri et al. (2021) show short-term negative employment and wage impacts for hurricane affected counties in Puerto Rico between 1995 and 2017. Similarly, Deryugina et al. (2018) show a short-run decline in labour market outcomes following hurricane Katrina. However, labour demand in other sectors could arguably increase through an element of "creative destruction", whereby damaged sub-optimal infrastructure is replaced with superior technology in the rebuilding phase. In this regard, Groen et al. (2020) find an increase in regional employment for those industries that are reconstruction related following hurricanes Katrina and Rita in 2005.

While assessing the economic impact of wildfires from a general natural hazards perspective can provide considerable insights, as pointed out by McCaffrey (2004), wildfires are also characterised by features that make them unique compared to other natural disasters. For instance, wildfires can perform beneficial functions for ecosystems under certain scenarios (Holmes et al., 2008). Moreover, wildfires are often human induced in that socioeconomic factors, such as poverty, education, or illegal activity, can contribute to the probability of wildfire occurrence (Michetti and Pinar, 2019), resulting in potential damage that is more easily mitigated or exacerbated by policy measures (e.g., land management, fire prevention) compared to other environmental hazards (Borgschulte et al., 2020).

Importantly, wildfires are particularly atypical among natural hazards since property damage can oftentimes be substantially reduced if there is large investment in manpower and equipment as described in Baylis and Boomhower (2019). Hence, central to understanding the potential economic impact of wildfires is the response during the hazard event itself. More specifically, during relatively short-duration hazards (e.g., earthquakes, hurricanes, floods) the mitigating response choice set for the direct effects is limited temporally, while wildfires can be actively "fought" and often last for several days or even weeks. Hence, an abundance of resources, including direct suppression spending and contracted services, are often made available during the wildfire event (Davis et al., 2014). If a substantial part of the employed services and goods are provided locally, these measures can also have major indirect impacts on regional economies. From an econometric perspective these aspects that are peculiar to wildfires raise important endogeneity concerns when trying to causally identify the economic impact of wildfires compared to other environmental disaster settings.

While a considerable body of literature has studied the conceivably detrimental and immediate impact of wildfires (Morton et al., 2003; Stephenson et al., 2013; CCST, 2020), a small number of studies scrutinise their effect on traditional economic indicators, such as GDP and employment growth. The most relevant research in this area was conducted by Nielsen-Pincus et al. (2013) who examine large wildfire events in the Western United States (US) and find an increase in county-level employment growth of 1% during the quarters where fire suppression efforts took place, although the effect is heterogeneous with regard to county characteristics and economic sectors (Nielsen-Pincus et al., 2014). Furthermore, Borgschulte et al. (2020) report reduced earnings of approximately 0.04% over two years per additional smoke exposure day for the US.

Although the impact of wildfires on the labour market or on GDP growth has to date drawn little attention, two other research areas evaluating economic impacts of wildfires are better understood. On the one hand, the hedonic pricing literature demonstrates a predominantly negative effect on house prices of up to 20% following wildfires in the US (Nicholls, 2019). Furthermore, Mueller and Loomis (2014) document that although property values are negatively affected by wildfires, there is large variation across the distribution of house prices, while McCoy and Walsh (2018) find a short-lived negative effect on property values if a burn scar can be viewed from the house. On the other hand, negative economic effects related to fire induced smoke pollution suggest that there are substantial health costs as demonstrated by Kochi et al. (2012), Richardson et al. (2012), Burke et al. (2020), Johnston et al. (2021), and Tarín-Carrasco et al. (2021). However, even for these relatively well researched aspects of wildfires, the majority of studies focus on the US and Australia, and not on Europe.

The current study makes three main contributions to the literature. First, we examine the economic implications of wildfires on regional employment and GDP growth in Europe, which to the best of our knowledge has not been explored. Since wildfires in Europe are perceived as a growing risk that predominantly affects Southern Europe, our study provides some of the first evidence on economic impacts for this fire-prone geographical region. Second, we focus on small-scale regional effects, which Horwich (2000) argues are important because natural disasters are for the most part localised events, and potential impacts are often imperceptible when studied at more aggregated geopolitical levels. As a matter of fact, neglecting potential regional economic impacts has already been identified as a major shortcoming of most previous studies addressing the impacts of natural hazards (Botzen et al., 2019).

Table 1
Sample composition and descriptive statistics showing the size of NUTS 3 regions by country.

	N	Proportion (%)	Mean (km^2)	sd (km^2)	Median (km^2)
Portugal	23	10	3,860	1,948	3,345
Spain	52	22	9,588	5,251	9,317
Italy	106	46	2,774	1,679	2,454
Greece	52	22	2,534	1,706	2,339

Notes: (i) Proportion (%) = the number of regions per country as a share of all sample regions; (ii) sd = standard deviation.

Third, in order to overcome potential endogeneity concerns when empirically estimating the economic effect of wildfires, we employ a novel causal identification strategy creating an instrumental variable (IV) by isolating climatic features for predominantly forested areas that are particularly relevant for capturing the probability of wildfire occurrence while also controlling for general and related climate conditions that might affect regional economic outcomes directly.

The empirical analysis in this paper relies on the construction of a panel data set matching annual regional economic data on employment and GDP growth from 2010 to 2018 with burned area (BA) polygons based on satellite imagery for regions in Portugal, Spain, Italy, and Greece. These data are combined with general climatic data, land cover maps, and a time-varying Fire Weather Index (FWI). Employing two-stage least squares (2SLS) instrumental variables regressions arguably allows us to causally quantify any potential effects of wildfires on annual regional employment and GDP growth in Southern Europe over our sample period.

To briefly summarise our results, we find an annual decrease in the rate of GDP growth of 0.11–0.18% for wildfire affected regions. Given that 102 regions are affected by wildfires every year on average, our findings indicate rough annual economic losses for Southern Europe in the range of 13–21 billion euros. There is also a heterogeneous impact on employment growth across economic activities where annual employment growth in tourism-related activities (e.g., accommodation, transportation, food service) decreases by 0.09–0.15%, while the sectors that include financial, insurance, real estate, and administrative activities experiences an average increase in the employment growth rate of 0.13–0.22%.

The remainder of the paper is organised as follows. Section 2 describes the data sources, how we constructed variables, and provides some descriptive statistics. Section 3 describes our identification strategy, the instrument construction, and econometric specification. Finally, the results are presented and discussed in Section 4 while Section 5 concludes.

2. Data and descriptive statistics

2.1. Regional unit of analysis and sample composition

The Nomenclature of Territorial Units for Statistics (NUTS) classification provides harmonised regional statistics for the European Union member and partner states. The hierarchical system divides the economic territory into major socio-economic regions (NUTS 1), basic regions for the application of regional policies (NUTS 2), and small regions for specific diagnoses (NUTS 3). Our countries of interest include a total of 243 NUTS 3 regions, namely 25 *Entidades Intermunicipais* for Portugal, 59 *Provincias* for Spain, 107 *Provincie* for Italy, and 52 *Omades Periferiakon Enotition* for Greece (Eurostat, 2020). For data availability and comparability reasons the following regions are excluded from our analysis: The Azores and Madeira for Portugal (2 regions), the Canary Islands for Spain (7 regions), and Sud Sardegna for Italy (1 region) leaving 233 NUTS 3 regions that are used in our analysis.[2]

Table 1 shows the sample composition and the disaggregated mean and median size of the NUTS 3 regions by countries. Italy accounts for almost half of the regions (46%), Spain and Greece each add up to about one fifth, and one in ten regions is in Portugal. One can observe variation in the mean size of a unit per country, with the largest regions in Spain, and the smallest in Italy and Greece, on average.

2.2. Economic data

We use data on regional level employment and per capita GDP as provided by the regional economic accounts of the Statistical Office of the European Union (Eurostat).[3] Regional accounts are derived from the corresponding national accounts, and thus, are generally defined using the concepts applied to national accounting procedures.[4] The estimation of regional GDP can follow either the production or the income approach.[5] The production approach measures regional GDP as the sum of gross value added (GVA), which is defined as the difference between output and intermediate consumption, plus taxes minus product subsidies. For the income

[2] The omissions for Portugal and Spain are due to missing meteorological and Fire Weather Index data, and the excluded Italian region is due to rearranged regional boundaries during the study period.

[3] https://ec.europa.eu/eurostat/web/rural-development/data (accessed in August 2021).

[4] It is noteworthy that a series of conceptual and practical difficulties arise when breaking down national data or compiling regional data directly. Challenges in accurate regional estimations involve how to account for enterprises with several regional establishments, extra-regio territory, major construction projects, cross regional boundary pipelines and cable distribution networks, or commuter flows, to name a few. For a detailed discussion with accompanying guidelines, see Chapter 13 in Eurostat (2013a) and Eurostat (2013b).

[5] Unlike for national data, the expenditure method cannot be applied given the absence of data on imports and exports on the regional level.

Table 2
Statistical classification of economic activities in the European community (NACE).

Category	Section	Description
A	A	Agriculture, forestry and fishing
B–E	B	Mining and quarrying
	C	Manufacturing
	D	Electricity, gas, steam and air conditioning supply
	E	Water supply, sewerage, waste management and remediation activities
F	F	Construction
G–J	G	Wholesale and retail trade; repair of motor vehicles and motorcycles
	H	Transportation and storage
	I	Accommodation and food service activities
	J	Information and communication
K–N	K	Financial and insurance activities
	L	Real estate activities
	M	Professional, scientific and technical activities
	N	Administrative and support service activities
O–U	O	Public administration and defence; compulsory social security
	P	Education
	Q	Human health and social work activities
	R	Arts, entertainment and recreation
	S	Other service activities
	T	Activities of households as employers
	U	Activities of extraterritorial organisations and bodies

approach, regional GDP at basic prices is derived from measuring and aggregating the regional generation of income of the economy, i.e., wages and salaries, the sum of other taxes minus subsidies on production, employers' social contributions, gross operating surplus, and consumption of fixed capital. In practice, gross operating surplus is generally not available by region and industry which poses a barrier to using the income approach. In general, countries are free to choose their preferred estimation approach. Hence per capita figures can be calculated for all regions excluding extra-regio measures (Eurostat, 2013b).

Our measure of regional employment is from the European Union Labour Force Survey that is based on a household sample survey of people aged 15 years and over. Persons are categorised as "employed" if any work has been performed during the survey reference week (e.g., for pay or family gain) or if they had a job at the time but were temporarily absent due to illness, holidays or educational training. The aggregated annual average of employed persons makes allowance for the fact that some people are not employed over the entire year but do casual or seasonal work (Eurostat, 2013b). Using the population data provided by Eurostat we calculate the share of employed persons in the total population.[6] We are also able to disaggregate employment growth by sections based on the Statistical classification of economic activities in the European Community (NACE) Rev.2, which is a revised classification implemented in 2007.[7] More specifically, we use Eurostat data for six categories that combine and classify a total of 21 individual economic activity sections as shown in Table 2 (Eurostat, 2008).

The regional economic variables are available from 2010 to 2018 and we use first differences of their logged values (i.e., growth rates) in our analysis. The geographical distribution of the average yearly employment and GDP growth rates across the NUTS 3 regions is shown in Fig. 1. The maps demonstrate that while the distribution of the employment growth rate (Fig. 1(a)) is fairly heterogeneous across countries, with intra-country regions experiencing both positive and negative employment growth rates over the study period, the emerging image for the GDP growth rates is strikingly different (Fig. 1(b)). Rather we observe clear differences at the country-level, indicating predominantly positive GDP growth in Portugal, Spain, and Italy, and negative growth in Greece.[8]

Descriptive statistics for the economic variables are summarised in Table 3. On average, 39.6% of the population is employed, and the employment growth rate is centred around zero with a slight tendency towards being positive. The smallest and largest values are within five standard deviations of the mean. The average per capita GDP is 21,184 euros, and on average positive GDP growth rates over the time period are observed. The GDP growth rates are within around six standard deviations of the mean.

2.3. Wildfire impact variables

The impact of wildfires is proxied by fire numbers as an absolute measure, and BA as a share of a region's total area. The primary data set for the construction of these variables is the high-resolution harmonised spatial BA data product provided by the European Forest Fire Information System (EFFIS).[9] This data product is based on a semi-automatic approach that combines Moderate Resolution Imaging Spectroradiometer (MODIS) satellite imagery with two bands (red and near-infrared) at a 250 meter spatial

[6] https://appsso.eurostat.ec.europa.eu/nui/show.do?dataset=nama_10r_3popgdp&lang=en (accessed in August 2021).
[7] Derived from French, NACE translates as Nomenclature statistique des activités économiques dans la Communauté européenne.
[8] Note, that our study period starts shortly after the financial crisis where Greece was particularly hard hit.
[9] https://effis.jrc.ec.europa.eu (accessed in July 2021).

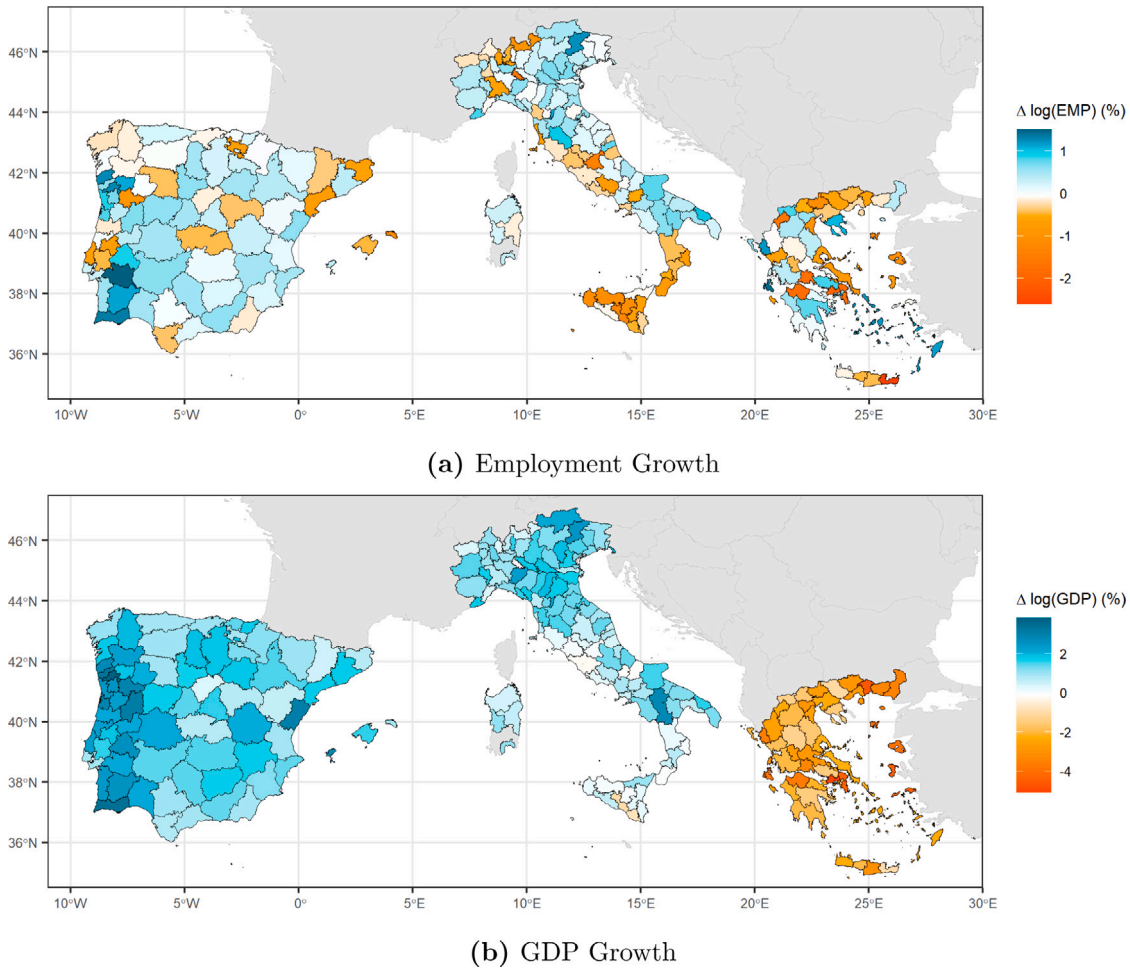

Fig. 1. Average annual employment and GDP growth rates (2011–2018).
Notes: (i) economic data are from the Statistical Office of the European Union (Eurostat); (ii) Δlog(EMP) denotes the growth of the employment rate and Δlog(GDP) is the per capita GDP growth rate.

Table 3
Descriptive statistics of economic variables (2010–2018).

	Min	Mean	sd	Median	Max	N
Employed/total population (%)	24.6	39.6	6.3	39.7	67.6	2,097
Δlog(EMP) (%)	−12.3	0.0	2.6	0.3	12.8	1,864
GDP/capita (€)	9,500	21,184	7,268	19,600	55,900	2,097
Δlog(GDP) (%)	−20.0	0.4	3.8	1.0	22.5	1,864

Notes: (i) economic data are from the Statistical Office of the European Union (Eurostat); (ii) Δlog(EMP) denotes the growth of the employment rate and Δlog(GDP) is the per capita GDP growth rate; (iii) sd = standard deviation.

resolution,[10] ancillary spatial data sets, and refinement of the perimeters through visual inspection backed up by news coverage. The burn perimeters are updated up to two times a day capturing fires larger than around 30 hectares.[11] In order to analyse potential lagged effects on the economic outcome variables our study includes all fires from 2001 to 2018.

[10] There are five bands (blue, green, as well as three short-wave infrared bands) with spatial resolution of 500 meters that help to improve BA discrimination by providing complementary information.
[11] https://effis.jrc.ec.europa.eu/about-effis/technical-background/rapid-damage-assessment (accessed in July 2021).

Table 4
Descriptive statistics of wildfire impact variables and the Fire Weather Index (2010–2018).

	Min	Mean	sd	Median	Max	N
All observations						
FIRE	0	3	9	0	129	2,097
BA (%)	0	0.34	1.53	0	33.82	2,097
Wildfire affected observations						
FIRE	1	7	13	2	129	920
BA (%)	0.001	0.77	2.24	0.13	33.82	920
Instrument						
FWI forest	0.0	15.9	11.6	14.9	64.8	2,097

Notes: (i) FIRE indicates the annual number of wildfires per region; BA in % denotes the annual burned area relative to the total area per region; FWI forest indicates the daily mean Fire Weather Index over the summer months for predominantly forested areas; (ii) "Wildfire affected observations" includes all observations where at least one wildfire occurred in a given year; (iii) sd = standard deviation.

For cross-border wildfires that affect several regions, the burn perimeters are split according to the NUTS 3 regional boundaries.[12] We exclude all fires that burned less than five hectares after the splitting process from the fire count variable, while all burned area counts towards the BA variable. Between 2010 and 2018 the number of wildfires in the dataset is 6709, whereby less than 1% resulted from the splitting process by regions. The total area burned over this period is approximately 2.4 million hectares.

The wildfire impact proxy variables are summarised in Table 4 for 2010 to 2018.[13] The mean fire number for all regions is three, and an annual average of 0.3% of a region is burned. Only considering the observations that experienced at least one fire denoted as "wildfire affected observations", the mean fire number is seven with an average of approximately 0.8% of total area burned. In our sample, one or more wildfires occurred in about 44% of the observations, and 82% of the regions were affected over the study period. On average about a third of the regions (30%) experience a wildfire each year.

Regarding the spatial distribution of the average annual wildfire numbers shown in Fig. 2(a), most fires are observed in Southern Italy and in the Northwest of the Iberian Peninsula. Focusing on the BA (proportional to the total area of a region) displayed in Fig. 2(b), the highest values are in Central and Northern Portugal. Fig. 2(c) shows the average wildfire size in hectares for each region over the study period. In contrast to Fig. 2(a) and Fig. 2(b), there are comparably low values for Italy and large values for the average fire size in Greece.

2.4. Fire weather index (FWI)

The FWI is a component of the Canadian Forest Fire Weather Index System initially introduced by Van Wagner and Pickett (1985). Fig. 3 presents a schematic of the FWI structure. The FWI captures relative fire potential, and serves as primary reference index to the Joint Research Centre (the European Commission's science and knowledge service) in the production of fire danger maps (Camia et al., 2008). The FWI is based on the combination of the two fire behaviour indices (1) Initial Spread Index (ISI) and (2) Buildup Index (BUI). The ISI estimates fire spread potential by integrating the Fine Fuel Moisture Code (FFMC), which is intended to represent fuel moisture conditions for litter fuels shaded by the forest canopy, and surface wind speed (u and v components).[14] The BUI provides information on potential heat release incorporating fuel moisture information from deeper soil layers. More specifically, it combines the Duff Moisture Code (DMC) capturing decomposed organic material below the litter fuels, and the Drought Code (DC) representing the moisture content of the deep compact layer assessing seasonal drought effects on heavy fuels. Both the DMC and the DC are adjusted for day-length of the month.

As can be seen from Fig. 3, the basic climatic inputs underlying the construction of the FWI are temperature, relative humidity, wind speed, and precipitation. All variables are measured at solar noon standard time. Precipitation is an accumulated measure over 24 h. The details of the construction from the initial meteorological observations to the derivation of the fire behaviour indices ISI and BUI are beyond the scope of this paper, but are described in Van Wagner and Pickett (1985). However, we do provide an outline of the calculations for the fire behaviour indices for the FWI in Appendix A.

We use the daily FWI calculated by Natural Resources Canada presented in McElhinny et al. (2020). The primary meteorological inputs are from the European Centre for Medium-Range Weather Forecasts (ECMWF) ERA5 HRES reanalysis product with a spatial resolution of 0.25° (approximately 27–28 kilometres in our latitudes of interest).[15] We work with the FWI version using the overwintered DC, which captures inter-seasonal drought. This is preferable to using a default start value as the overwintered DC is more precise accounting for precipitation in the winter months.

[12] The NUTS 2016 version of the shapefile scaled 1:1 million is provided by Eurostat at https://ec.europa.eu/eurostat/web/gisco/geodata/reference-data/administrative-units-statistical-units/nuts is used (accessed in July 2021).

[13] Although we have data from 2001 to 2018 we display the descriptive statistics for the period that matches the economic outcome variables since these figures are later used to interpret the regression coefficients.

[14] u is the component of the horizontal wind towards east (zonal velocity) and v denotes its counterpart towards north (meridional velocity).

[15] Note, the primary resolution of ERA5 is 0.28125° on a reduced Gaussian grid, but the output on a regular geographical grid is 0.25°.

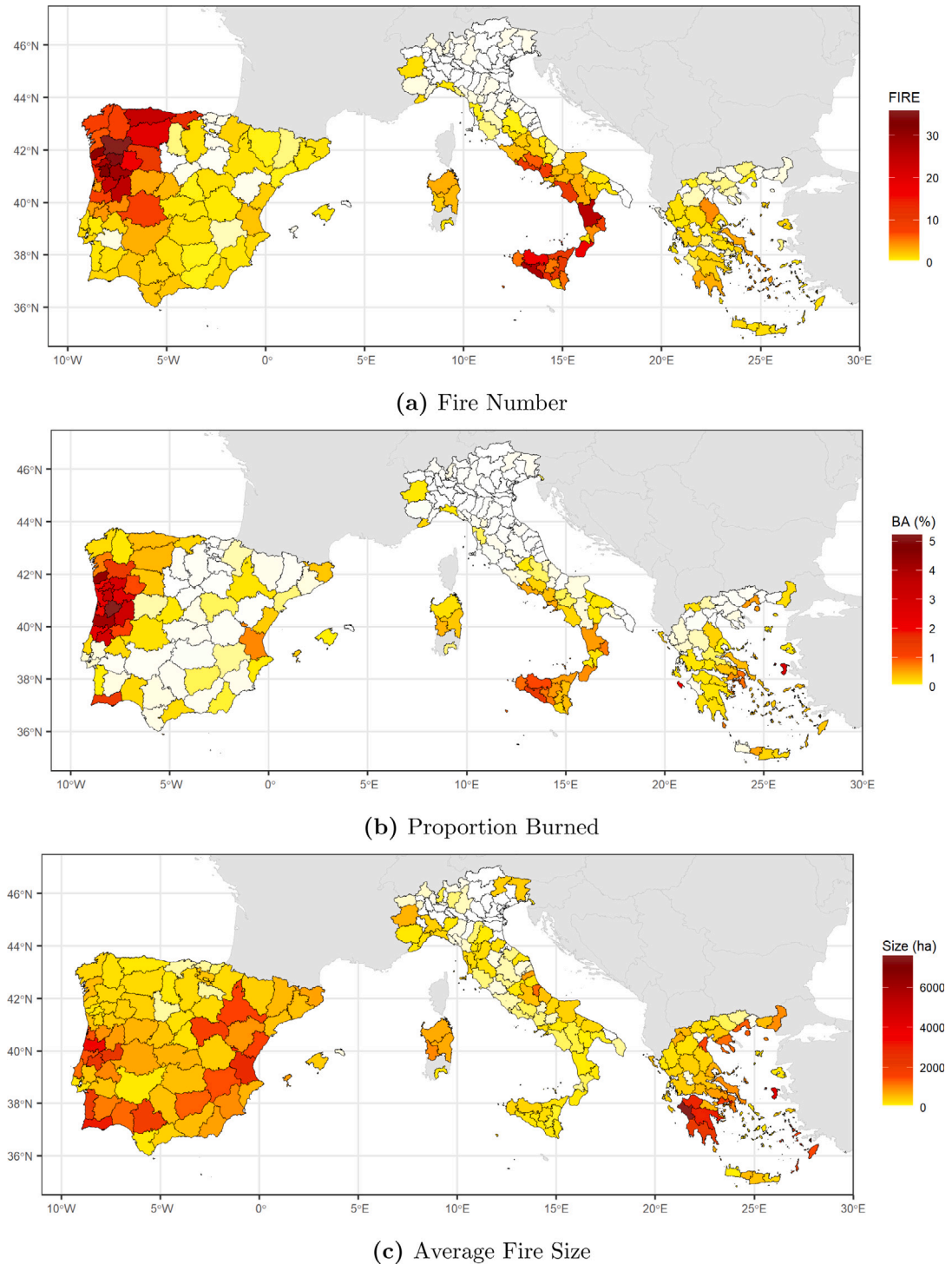

Fig. 2. Average annual wildfire occurrence (2010–2018).
Notes: (i) wildfire data is taken from a high-resolution burned area product provided by the European Forest Fire Information System (EFFIS); (ii) FIRE indicates the annual number of wildfires per region; BA in % denotes the annual burned area relative to the total area per region; Size indicates the average size of a fire in hectares (ha).

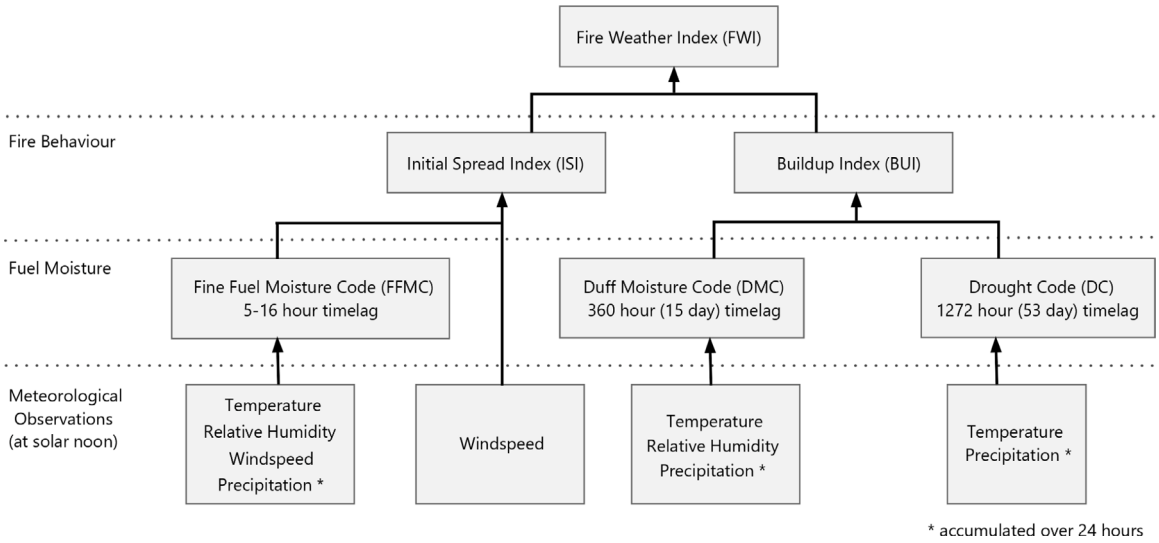

Fig. 3. Structure of the Canadian Fire Weather Index System based on Van Wagner and Pickett (1985).

2.5. Land cover data

We resort to the CORINE land cover (CLC) data provided by the Copernicus Land Monitoring Service in order to distinguish between forested and non-forested areas within the studied regions.[16] CLC is specified to standardise land cover data collection in order to support environmental policy development. It was initialised in 1990 and is updated every six years. While orthocorrected satellite images provide the basis for the land cover mapping, ancillary information such as in-situ and ground survey data enhance accuracy.[17] The minimum mapping unit/width is 100 m (25 hectares) with a thematic accuracy exceeding 85%. The CLC inventory comprises 44 land cover types (European Environment Agency, 2021).

We use the raster files of the years 2006 and 2012 and reclassify the 44 land cover types into four suitable categories for our study purposes, namely urban areas (i.e., artificial surfaces), agricultural areas, forested areas (including forests as well as shrub and/or herbaceous vegetation), as well as wetlands and water bodies (also including open spaces with little or no vegetation). See Table B1 in Appendix B for the exact reclassification.

2.6. Climatological data

Temperature, precipitation, and relative humidity data are taken from the E-OBS, a daily gridded meteorological data set for Europe with a spatial resolution of 0.25° and is derived from in-situ observations based on the station network of the European Climate Assessment & Dataset (ECA&D) project.[18] Temperature is measured in degrees Celsius at a height of two metres and daily precipitation consists of the total amount of rain, snow, or hail (equivalent to the height in liquid water per square meter) in millimetres. Daily averaged relative humidity in percentage is based on the observational station time series from ECA&D. In order to remove data skewness, the relative humidity values are transformed by $\sqrt{100 - relative\ humidity}$ before the fitting process to ensure all interpolated values are equal or smaller than 100 when converted to percentages.

For every NUTS 3 region, we take the following approach to calculate seasonal and annual average temperature, precipitation, and relative humidity for each of the four land cover type categories (i.e., urban, agriculture, forest, wetland and water bodies). First, an E-OBS gridcell for a specific land cover type is matched with a region if, in the overlapping part of the region and the E-OBS gridcell, a majority of the area is of that specific land cover type. Second, we average all the E-OBS gridcell values that are matched for a specific region and land cover type. Third, we use the daily meteorological data to calculate seasonal, i.e., summer months, and annual average temperature, precipitation and relative humidity for each of the four land cover types.

Even though the E-OBS data set provides information on wind speed, there are many missing values, particularly for Southern Greece and Sicily. Therefore, we instead use the 10 meter u and v wind components from the fifth generation of the ECMWF atmospheric reanalyses of the global climate (ERA5) data product (Hersbach et al., 2020). The spatial resolution of 0.25° is similar to the E-OBS data set and the temporal resolution is hourly. We extract daily values at 12 pm and match the ERA5 gridcells with

[16] https://land.copernicus.eu/pan-european/corine-land-cover (accessed in August 2022).

[17] Both the 2006 and the 2012 versions are based on the Indian Remote-Sensing Satellite P6 LISS III and on the dual date satellites (Sentinel-2 and Landsat 8). SPOT-4/5 is additionally used for year 2006 and RapidEye Earth-imaging Systems for year 2012.

[18] For details see Cornes et al. (2018).

the NUTS 3 regions for each land cover type in a similar manner as described for the other climatic variables. Once processed to seasonal and annual average values, wind speed is calculated from the u and v component where $wind\ speed = \sqrt{u^2 + v^2}$.

3. Empirical framework

3.1. Identification strategy

The identification of the causal effect of wildfires on regional economies is complicated by the potential endogeneity of the wildfire proxy impact variables. As we employ geophysical measures, i.e., remotely sensed imagery defining the BA, in conjunction with regional level fixed effects, the source of endogeneity typically induced by using reported loss or damage data (e.g., through insurance claims that are likely to correlate with GDP/capita) is avoided, as outlined in Felbermayr and Gröschl (2014). However, using ordinary least squares (OLS) with regional level fixed effects, even with the geophysical based measures of the fires, might still produce biased estimates due to a number of time varying unobserved factors. Regional unobservables include, inter alia, fire and land management policies (e.g., fire prevention and suppression regimes), rural exodus/urbanisation rates, land-use changes (e.g., deforestation), land-use regulations, political instability, and local government corruption. These endogeneity concerns are particularly important for wildfires as opposed to other natural disasters because wildfires are often due to human induced activities (under the right climatic conditions) and are generally not instantaneous events.

The likely direction of bias for the aforementioned factors will differ depending on which unobservable one is considering. If the unobservable is negatively correlated with wildfire occurrence and positively correlated with the economic outcome variables or vice versa, we expect a downward bias of the OLS estimate. For example, one might expect wildfires to be reduced if a region implements effective fire prevention measures (e.g., mechanical clearing of land, fire breaks, grazing, educational campaigns), but at the same time employment may be increased as workers are needed to carry out these interventions. Likewise, urbanisation may coincide with a larger demand for fire services, which may also increase employment and hence reduce the BA as there are more locally available suppression resources. Turning to land-use changes, if the change is from forested to agricultural land (deforestation), this is likely to increase economic activity as it might be a more profitable use of land and would also decrease wildfires which generally occur in forested areas. A downward bias would also be observed for the case of political instability or corruption levels that lead to a potential increase in BA, e.g., around elections (Skouras and Christodoulakis, 2014) which could at the same time plausibly have a negative impact on economic activity.

One might also expect upward biased estimates if certain unobservables are taken into account that are positively correlated with both wildfire occurrence and employment/output. For example, a rural exodus would result in abandoned and unmanaged forests which potentially increases wildfire occurrence, but could also increase GDP growth if there are better job opportunities in regional economic centres. Furthermore, certain environmental regulations might create perverse incentives for arson (e.g., if the burned land can subsequently be used for cultivation or construction) so that the fire numbers potentially increase, quite possibly accompanied by the creation of employment and GDP growth if the land is repurposed towards more productive activities.

Finally, OLS estimates may suffer from classical measurement error, which leads to a bias towards zero introduced by measuring the BA using satellite data that is arguably imperfect. More specifically, the data is based on a multi-step process, which means that the data is heavily reliant on working instruments on board the satellites at all times, but also on visual inspection and manual processing. Both aspects could thus lead to attenuation bias. Moreover, as described in Alix-Garcia and Millimet (2021) and Garcia and Heilmayr (2022) using satellite data can induce non-classical (systematic) measurement error. More specifically, as noted in Section 2.3, not all fires smaller than 30 hectares are detected by the satellite. Therefore, the true BA might be marginally larger than in our data set. While Alix-Garcia and Millimet (2021) provide a solution if the data derived by remotely sensed imagery is used as the dependent variable in a regression, we are not aware of an applicable strategy if the independent variable is based on satellite data, as it is in our case. This thus constitutes a limitation of our study.

Our empirical strategy is to isolate time-varying fire danger for the predominantly forested areas in the summer months which is arguably a good predictor for wildfire occurrence (first stage). As described in Section 2.4, the FWI is based on meteorological inputs and can thus be considered as good as randomly assigned. Moreover, by construction the FWI arguably only picks up the distinctive part of the meteorological factors indicative of wildfire danger. In order to ensure the satisfaction of the exclusion restriction we implement two vectors of control variables. First, we also include the FWI in predominantly urban, agricultural, and wetlands and water body areas of a region. Second, we control for a battery of other climatic variables i.e., temperature, precipitation, relative humidity and wind speed within the region. Every climatic variable is created separately for each of the four land cover types and is included both as summer month averages and as annual averages. By including these additional control factors we are thus ensuring that our instrument is not capturing climatic factors affecting the non-predominantly-forested areas within a region that might affect economic activity other than through wildfire occurrence, such as, for example, through their impact on the agricultural sector (Damania et al., 2020).

Since the inputs into the FWI are also temperature, precipitation, relative humidity and wind speed, the FWI captures the remaining variation through the joint occurrence of specific threshold values and/or their non-linear transformations of these in its construction.[19] Moreover, some inputs into the FWI have a different time dimension. For example, the Drought Code input into

[19] For example, the Buildup Index, which forms part of the fire behaviour indices capturing heat release, is constructed of non-linear functions depending on whether today's Duff Moisture Code (denoted as P) is below are above 0.4 ∗ today's Drought Code (denoted as D) as shown in Eq. (4) in Appendix A. Subsequently the Buildup Index is used to calculate an intermediate form of the FWI, namely the duff moisture function, $f(D)$, which is once again derived from a non-linear function. More specifically, the duff moisture function is calculated as $0.626 * \mathrm{BUI}^{0.809} + 2$ if the Buildup Index is smaller or equal to 80, and as $1000(25 + 108.64e^{-0.023*\mathrm{BUI}})$ if the Buildup Index is larger than 80 as shown in Eq. (5) in Appendix A.

the FWI has a 53-day time lag and thus differs temporally from the precipitation and temperature in the general climate controls employed. Furthermore, the precipitation amount is adjusted to slope effects of the landscape. The Duff Moisture Code and the Drought Code are also adjusted for the day-length of the month (e.g., to account for the dry rate and potential evapotranspiration from the soil following rainfall), and thus go beyond using pure meteorological inputs in their elaborated construction designed for capturing fire danger. Our identifying assumption is thus that the instrument isolates the specific meteorological aspects leading to a substantially higher wildfire occurrence probability for predominantly forested areas conditional on controlling for fire danger in other areas that are arguably much less flammable, as well as for general climatological conditions within each of these area types.

3.2. Instrument construction

The FWI variable for forested area implemented as the instrument is created as follows. For the intersection of each region and FWI gridcell we tabulate the share of the four reclassified land cover types. To this end, we use the latest CLC version, i.e., the FWI years 2010–2012 are matched with CLC 2006 and the FWI years 2013–2018 are matched with CLC 2012. Each NUTS 3 region is then spatially joined with all the FWI gridcells that intersect with the region under the condition that the overlapping area is predominantly forested (> 50%). Subsequently, the average daily value of all matching FWI gridcells for each region is calculated. Finally, the daily mean FWI value for June, July, and August is calculated for each region as wildfires are most common in the summer months.[20] In our sample, the average FWI value for predominantly forested areas in the summer months is approximately 16 (see Table 4), which is described as "Moderate Fire Danger" according to the EFFIS classification[21] based on Van Wagner and Pickett (1985).[22]

3.3. Econometric specification

We evaluate the potential impact of wildfires on two economic variables in first differences, namely on the growth of the employment rate $\Delta\log(\text{EMP})$ over $t-1$ to t defined as $\log(\text{employed/total pop})_{i,t} - \log(\text{employed/total pop})_{i,t-1}$, and on the GDP growth rate $\Delta\log(\text{GDP})$ over $t-1$ to t defined as $\log(\text{GDP/capita})_{i,t} - \log(\text{GDP/capita})_{i,t-1}$, where i represents a NUTS 3 region and $t = [2011, \ldots, 2018]$.

We estimate the following fixed effects 2SLS linear panel model instrumenting the fire impact variables with the FWI for predominantly forested areas:

$$\text{IMPACT}_{i,t-1\to t} = \beta_1 \text{FWI forest}_{i,t-1} + \mathbf{OFWI}_{i,t-1}\boldsymbol{\gamma}_1 + \mathbf{C}_{i,t-1}\boldsymbol{\delta}_1 + \pi_t + \mu_i + \varepsilon_{i,t} \tag{1}$$

$$\Delta\text{ECON}_{i,t-1\to t} = \beta_2 \widehat{\text{IMPACT}}_{i,t-1} + \mathbf{OFWI}_{i,t-1}\boldsymbol{\gamma}_2 + \mathbf{C}_{i,t-1}\boldsymbol{\delta}_2 + \pi_t + \mu_i + \varepsilon_{i,t}, \tag{2}$$

where $\text{IMPACT}_{i,t-1\to t}$ is a placeholder for the wildfire impact proxy variables, fire numbers or BA, $\text{FWI forest}_{i,t-1}$ is the daily mean Fire Weather Index in the summer months for predominantly forested areas, $\mathbf{OFWI}_{i,t-1}$ is a vector of the FWI for the other areas i.e., predominantly urban areas, rural areas, as well as for wetlands and water bodies in the summer months. Thereby, the FWI for the other land cover types are constructed similarly to the FWI for predominantly forested areas explained in Section 3.2. Moreover, $\mathbf{C}_{i,t-1}$ represents a vector of climatological controls including average summer and annual temperatures, precipitation, relative humidity, and wind speed. All the climatic controls are also implemented for each of the four land cover types separately and are created similarly to the land cover specific FWI variables explained in Section 3.2. π_t and μ_i account for unobserved year and regional fixed effects, respectively, and $\epsilon_{i,t}$ are idiosyncratic errors. $\Delta\text{ECON}_{i,t-1\to t}$ is alternatively defined by either $\Delta\log(\text{EMP})_{i,t-1\to t}$ or $\Delta\log(\text{GDP})_{i,t-1\to t}$, and $\widehat{\text{IMPACT}}_{i,t-1}$ is the predicted value of the wildfire impact variables in Eq. (1).

As our unit of analysis is at the regional level, one may worry about spatial correlation across regions. More specifically, the degree of economic integration between regions is likely to increase with geographical proximity and thus economic shocks may be spatially correlated. Hence we estimate our regression models with heteroskedasticity and autocorrelation consistent (HAC) standard errors that are robust to spatial correlation.[23] The necessary geospatial inputs for the estimation of spatial HAC standard errors are created using the longitude and latitude of the region's centroids. We choose a distance threshold for spatial correlation that corresponds to the radius of the NUTS 3 region's median area presuming a circular form of a unit, and add approximately 10% to this value which results in 33 km, in order to ensure that we include adjacent regions in the spatial correlation matrix.

We also explore whether there is a lagged impact of wildfires on regional economic outcomes by including up to $t-1-z$ lagged values of the IMPACT variable in Eq. (2). Note that in terms of instrumenting for these lagged values we do not use the complete set of lagged FWI variables in a joint 2SLS estimation framework because it would not be appropriate to expect $t-1-z$ values of FWI to be predictors for $t-1-z+n, n = 1, ..N$ values of IMPACT. Instead we estimate Eq. (1), generate the predicted values $\widehat{\text{IMPACT}}_{i,t-1}$, and include these and lagged values thereof in Eq. (2). However, as the contemporary and lagged values of the predicted $\widehat{\text{IMPACT}}_{i,t-1}$

[20] https://climate.copernicus.eu/esotc/2020/wildfires (accessed in December 2021).

[21] https://gwis.jrc.ec.europa.eu/about-gwis/technical-background/fire-danger-forecast (accessed in August 2021).

[22] See Table B2 in Appendix B for the complete classification of the FWI ranges.

[23] To test spatial correlation, we use Moran's I introduced by Moran (1950) and proposed by Cliff and Ord (1972). We implement a row-standardised inverse distance weight matrix. The null hypothesis of uncorrelated residuals is rejected for all combinations for both dependent variables and years. Hence, we implement spatial HAC standard errors.

Table 5
Wildfires and employment growth (2011–2018).

	Δlog(EMP)		FIRE	BA	Δlog(EMP)		
	(1)	(2)	(3)	(4)	(5)	(6)	(7)
FIRE $\times 10^{-2}$	−0.005					0.044	
	(0.005)					(0.055)	
BA		0.040					0.240
		(0.046)					(0.307)
FWI forest			0.370***	0.067*	0.000		
			(0.107)	(0.027)	(0.000)		
Climate Ctrl	Yes	Yes	Yes	Yes	Yes	Yes	Yes
FWI Ctrl	Yes	Yes	Yes	Yes	Yes	Yes	Yes
Fixed Effects	Yes	Yes	Yes	Yes	Yes	Yes	Yes
R^2	0.30	0.30	0.60	0.31	0.40	0.39	0.39
Model	OLS	OLS	1st stage	1st stage	Reduced	IV	IV

Notes: (i) * p <0.05, ** p <0.01, *** p <0.001; (ii) spatial HAC standard errors in parentheses as implemented by Foreman (2020) with a distance cutoff value of 33 km; (iii) N = 1864; (iv) the first stage F-statistics of 37 and 23 for fire numbers (Column (3)), and burned area (Column (4)), respectively, indicate that a weak instrument problem can be excluded (Stock et al., 2002); (v) Δlog(EMP) denotes the growth of the employment rate; FIRE is the annual number of fires (stated in 100 fires); BA is the proportion of the annual burned area per region; FWI forest denotes the mean of the daily Fire Weather Index in the summer months for predominantly forested areas; (vi) FWI controls include the Fire Weather Index for predominantly urban and agricultural areas as well as for wetlands and water bodies; climate controls include summer and annual means of the variables temperature, precipitation, relative humidity, and wind speed for each of the four land cover type categories separately; fixed effects include regional and time fixed effects.

will have their own distribution, using spatial HAC standard errors would no longer be appropriate. Were spatial correlation not an issue one could instead simply generate bootstrapped standard errors. Unfortunately, there is of date no accepted method to incorporate spatial correlation into standard bootstrapping procedures. We did experiment with 1000 re-sampled data sets using 2, 3, and 10-fold cross validation which preserved the spatial error structure. Yet, this resulted in unreasonably small standard errors, as upholding the spatial structure led to limited variation among the data sets.[24] Our solution is thus instead to implement HAC bootstrapped standard errors (1000 replications) in the lagged estimations without being able to take account of spatial correlation. Therefore, the lagged impact findings should be interpreted cautiously.

4. Results and discussion

4.1. Contemporary impact

In the first two columns of Table 5 we present the non-instrumented impact of our two wildfire proxies on employment growth, i.e., Eq. (2) but with direct measures of IMPACT rather than their instrumented counterparts. The results suggest there has been no significant impact of wildfires on aggregate employment growth during our sample period.

Columns (3) and (4) indicate that the estimations of Eq. (1) yield a strong first stage showing that the FWI for predominantly forested areas is a positive and statistically significant determinant of the wildfire impact variables at the 0.1 percent level for fire numbers and at the 5 percent level for BA. The positive effect meets a priori expectations since a higher fire danger index value arguably leads to more favourable conditions for both the outbreak and spread of wildfires. The effect size indicates an average increase of 0.4 fires per unit increase of the FWI (Table 5 Column (3)). An F-statistic of 37 for fire numbers indicates that a weak instrument problem can be excluded (Stock et al., 2002). Moreover, a unit increase of the FWI is associated with an increased share of BA of 0.007 percentage points (Table 5 Column (4)). The F test of joint significance in the first stage is 23 for BA, also indicating no weak instrument problem. Furthermore, the reduced form estimates displayed in Column (5) does not suggest an effect of the FWI for predominantly forested area on employment growth (Table 5).

The results of the IV estimations stated in Eq. (2) show a positive insignificant effect of the wildfire impact proxy variables on the growth of the employment rate. Thus, like previous research conducted in the US by Nielsen-Pincus et al. (2013) who report a general positive effect of large wildfires on employment growth of approximately 1% during the quarter of the fire at the regional (county) level, we find a positive effect for Southern Europe. However, it is not significant possibly because our study differs in that (i) we look at annual vs. their quarterly data, and thus a potential seasonal effect would not be detected, (ii) we include all fires, and therefore evaluate an aggregate effect, while Nielsen-Pincus et al. (2013) evaluate only large wildfire events,[25] and (iii) wildfires are on average much larger in the US than in Europe, and the resulting effect might thus be different.

Table 6 shows the effect of the wildfire proxy variables on GDP growth. The OLS results displayed in Columns (1) and (2) show a negative insignificant impact of wildfires on this economic activity indicator.[26] Unlike for aggregate employment, we find

[24] The standard errors for the 2-fold cross validation are about one quarter of the spatial HAC standard errors of the contemporary time period estimations.
[25] Thereby, a wildfire is defined as large when suppression spending exceeds one million US$.
[26] Columns (3) and (4) which show the first stage are identical to Table 5 and are reported for completeness.

Table 6
Wildfires and GDP growth (2011–2018).

	Δlog(GDP)		FIRE	BA	Δlog(GDP)		
	(1)	(2)	(3)	(4)	(5)	(6)	(7)
FIRE $\times 10^{-2}$	−0.005					−0.259*	
	(0.006)					(0.107)	
BA		−0.001					−1.425*
		(0.036)					(0.687)
FWI forest			0.370***	0.067*	−0.001***		
			(0.107)	(0.027)	(0.000)		
Climate Ctrl	Yes	Yes	Yes	Yes	Yes	Yes	Yes
FWI Ctrl	Yes	Yes	Yes	Yes	Yes	Yes	Yes
Fixed Effects	Yes	Yes	Yes	Yes	Yes	Yes	Yes
R^2	0.45	0.45	0.60	0.31	0.54	0.38	0.28
Model	OLS	OLS	1st stage	1st stage	Reduced	IV	IV

Notes: (i) * p <0.05, ** p <0.01, *** p <0.001; (ii) spatial HAC standard errors in parentheses as implemented by Foreman (2020) with a distance cutoff value of 33 km; (iii) N = 1864; (iv) the first stage F-statistics of 37 and 23 for fire numbers (Column (3)), and BA (Column (4)), respectively, indicate that a weak instrument problem can be excluded (Stock et al., 2002); (v) Δlog(EMP) denotes the growth of the employment rate; FIRE is the annual number of fires (stated in 100 fires); BA is the proportion of the annual burned area per region; FWI forest denotes the mean of the daily Fire Weather Index in the summer months for predominantly forested areas; (vi) FWI controls include the Fire Weather Index for predominantly urban and agricultural areas as well as for wetlands and water bodies; climate controls include summer and annual means of the variables temperature, precipitation, relative humidity, and wind speed for each of the four land cover type categories separately; fixed effects include regional and time fixed effects.

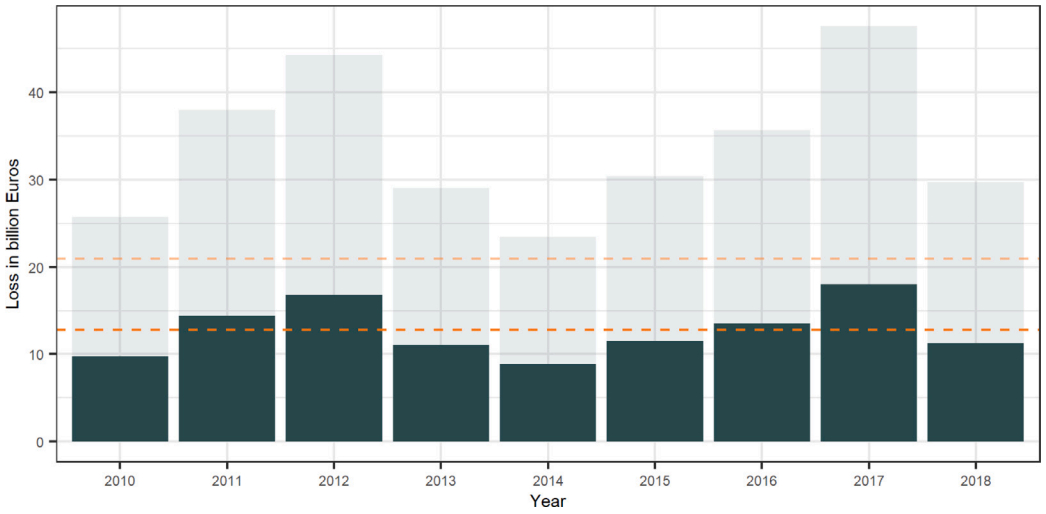

Fig. 4. Annual loss estimates based on a decrease in GDP growth for Southern Europe in billion euros (2010–2018).
Notes: (i) the solid bars indicate the lower bound and the transparent bars the upper bound of the estimate; (ii) the orange lines indicate the annual average losses (lower and upper bound) for the entire time period with an average of 102 wildfire affected regions per fire season.

a negative significant effect of the FWI for predominantly forested areas at the 0.1 percent significance level in the reduced form (Table 6 Column (5)). Both wildfire impact variables show a significant negative impact on GDP growth in the IV estimations (Columns (6) and (7)). One should note that the short-term negative GDP growth effects for wildfire affected regions found here are in line with the majority of the general natural disaster studies discussed in the introduction.

The point estimates on IMPACT of the IV specification in Table 6 indicate that, on average, an additional fire leads to a decrease in the regional annual GDP growth rate of 0.026% (Column (6)). As shown in Table 4, the mean wildfire number of the affected observations is 7 and thus the average wildfire affected region experiences a yearly decrease in the GDP growth rate of 0.18% ($-0.00259 * 7 = -0.018$). The largest number of annual wildfire events in a region observed is 129. Therefore, for the most severely hit region in the "worst" observed year over our sample period this would lead to a decrease of the annual GDP growth rate of 3.3% ($-0.00259 * 129 = -0.33$). The wildfire proxy variable BA (Column (7)) is also positive and significant and suggests a decrease in a region's yearly GDP growth rate, on average, of 0.11% ($-1.425 * 0.0077 = -0.011$) conditional on having experienced at least one wildfire. Table 4 shows that for the most heavily affected region in the data set, the aggregated annual BA was 33.82%. In such an extreme year, the regional GDP growth rate is predicted to decrease by 4.8% ($-1.425 * 0.3382 = -0.48$).

To get a better understanding of what these changes in growth rates mean in monetary values we calculate annual average losses for Southern Europe. To this end we multiply our estimated GDP growth effects with the mean GDP/capita value of 21,184 euros

Table 7
Wildfires and employment growth for NACE activity categories A, BE, and F (2011–2018).

	Δ log(EMP^{A})		Δ log(EMP$^{B\text{-}E}$)		Δ log(EMP^{F})	
	(1)	(2)	(3)	(4)	(5)	(6)
FIRE $\times 10^{-2}$	0.069		0.050		0.002	
	(0.158)		(0.074)		(0.228)	
BA		0.380		0.273		0.010
		(0.866)		(0.422)		(1.257)
FWI Ctrl	Yes	Yes	Yes	Yes	Yes	Yes
Climate Ctrl	Yes	Yes	Yes	Yes	Yes	Yes
Fixed Effects	Yes	Yes	Yes	Yes	Yes	Yes
N	1,856	1,856	1,864	1,864	1,864	1,864

Notes: (i) * p <0.05; (ii) spatial HAC standard errors in parentheses as implemented by Foreman (2020) with a distance cutoff value of 33 km; (iii) Δlog(EMP) denotes the growth in the employment rate; (iv) the superscript refers to the NACE activity where A includes agriculture, forestry and fishing, B-E is industry except construction, and F indicates construction; FIRE indicates the annual number of fires (stated in 100 fires); BA is the proportion of the annual burned area per region; (v) FWI controls include the Fire Weather Index for predominantly urban and agricultural areas as well as for wetlands and water bodies; climate controls include summer and annual means of the variables temperature, precipitation, relative humidity, and wind speed for each of the four land cover type categories separately; fixed effects include regional and time fixed effects.

(as shown in Table 3) which implies an average loss of production of 23.3–38.1 euros/capita ($21,184 * 0.0011 = 23.3$ using BA and $21,184 * 0.0018 = 38.1$ using fire numbers). Subsequently, we multiply the average GDP/capita losses with the mean regional population of 538,000 to calculate the average loss in production for one affected region, which is 12.5–20.5 million euros. Fig. 4 shows the monetary losses due to lost production for each year derived by the multiplication of the per region estimate with the number of wildfire affected regions, and therefore shows the variation related to the severity and intensity of the fire seasons. The average number of affected regions from 2010 to 2018 is 102, which suggests that losses are in the region of 12.8–20.9 billion euros for Southern Europe in a given year.

4.2. Employment growth by economic activities

We next scrutinise the aggregate positive insignificant effect of wildfires on the growth of the employment rate in different economic activity categories to explore potential heterogeneous effects. To this end, the NACE economic activity sections are combined into six main categories as shown in Table 2.[27] The effects of categories A, B–E, and F are shown in Table 7, and the results of categories G–J, K–N, O–U are given in Table 8. Furthermore, the heterogeneous effects of wildfires on the growth of the employment rate by economic activity categories are visualised in Fig. 5, showing the point estimates and the 95% confidence intervals for each category. The impact of wildfires on the growth of the employment rate in agriculture, forestry and fishing (Table 7 Columns (1) and (2)), on industries other than construction (category B–E) (Table 7 Columns (3) and (4)), as well as on construction (Table 7 Columns (5) and (6)) is positive but insignificant. Furthermore, the results show an insignificant negative effect on sector O–U, that is public administration and defence, compulsory social security, education, human health and social work activities, arts, entertainment and recreation, and repair of household goods and other services (Table 8 Columns (5) and (6)).

We find that two employment categories are significantly affected by wildfires. First, there is a negative effect of wildfires on the employment growth rate in sector G–J, which includes wholesale and retail trade, transport, accommodation and food service activities, information and communication (Table 8 Columns (1) and (2)). This could indicate that employment activities related to retail and tourism (e.g., wholesale and retail trade; land, air, and water passenger transport; hotels, campgrounds, restaurants) are negatively affected. Once again, we multiply our estimates with the average fire numbers and BA which leads to a regional annual decrease in the rate of employment growth in category G–J of 0.09–0.15% ($-0.00213 * 7 = -0.015$ using fire numbers (Column (1)) and $-1.174 * 0.0077 = -0.009$ using BA (Column (2))) for wildfire affected regions.

We quantify the estimated results of wildfires on employment growth for the specific activity categories in terms of job numbers to enhance the understanding of this magnitude. On average, 62,519 people (28.8% of the working population) are employed in the retail and tourism sections G–J per region as shown in Table B3 in Appendix B. Our estimates translate into 56–94 jobs lost per affected region annually ($62,519 * 0.0009 = 56$ using BA and $62,519 * 0.0015 = 94$ using fire numbers). With 102 regions that experience a wildfire in an average year this leads to a loss of 5,712–9,588 jobs for Southern Europe in the employment activity sectors including retail, transportation, as well as accommodation and food service activities.

Our findings concur with previous studies looking at recreational activities and tourism related to wildfires. For example, Kim and Jakus (2019) evaluate tourist flows in response to wildfires studying national park visits in Utah. The authors find a decrease in tourism in four out of five national parks and suggest an annual loss of 31–53 jobs based on the estimated loss in labour income. Furthermore, Gellman et al. (2022) study the effect of wildfires and smoke exposure on more than 1000 campgrounds in the western US showing that 1 million visitors per year are affected and estimate a decline in campground use. Evidence of wildfires affecting tourism-related industries in Southern Europe is provided by Molina et al. (2019) who estimate the economic susceptibility of

[27] One should note that there is no information for category A for 1 region.

Table 8
Wildfires and employment growth for NACE activity categories G–J, K–N, and O–U (2011–2018).

	Δ log(EMP^{G-J})		Δ log(EMP^{K-N})		Δ log(EMP^{O-U})	
	(1)	(2)	(3)	(4)	(5)	(6)
FIRE $\times 10^{-2}$	−0.213*		0.308*		−0.107	
	(0.089)		(0.138)		(0.066)	
BA		−1.174*		1.695*		−0.591
		(0.519)		(0.817)		(0.417)
FWI Ctrl	Yes	Yes	Yes	Yes	Yes	Yes
Climate Ctrl	Yes	Yes	Yes	Yes	Yes	Yes
Fixed Effects	Yes	Yes	Yes	Yes	Yes	Yes
N	1,864	1,864	1,864	1,864	1,864	1,864

Notes: (i) * p <0.05; (ii) spatial HAC standard errors in parentheses as implemented by Foreman (2020) with a distance cutoff value of 33 km; (iii) Δlog(EMP) denotes the growth in the employment rate; (iv) the superscript refers to the NACE activity where G–J includes wholesale and retail trade, transport, accommodation and food service activities, information and communication, K–N is contains financial and insurance activities, real estate activities, professional, scientific and technical activities, administrative and support service activities, and O–U includes public administration and defence, compulsory social security, education, human health and social work activities, arts, entertainment and recreation, and repair of household goods and other services; FIRE indicates the annual number of fires (stated in 100 fires); BA is the proportion of the annual burned area per region; (v) FWI controls include the Fire Weather Index for predominantly urban and agricultural areas as well as for wetlands and water bodies; climate controls include summer and annual means of the variables temperature, precipitation, relative humidity, and wind speed for each of the four land cover type categories separately; fixed effects include regional and time fixed effects.

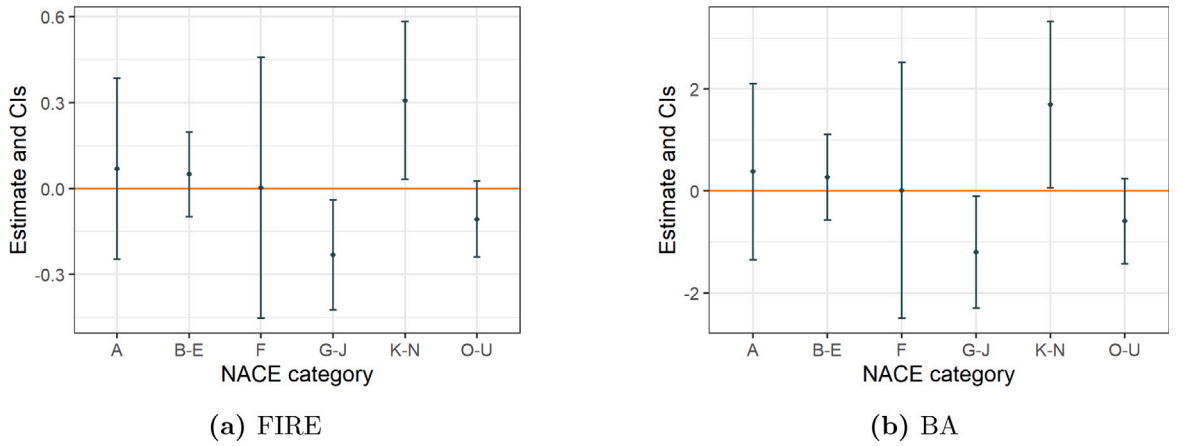

Fig. 5. Wildfires and employment growth by economic activity category (2011–2018).
Notes: (i) the economic activity categories are defined following the Statistical classification of economic activities in the European Community abbreviated as NACE (see Table 2 for the full NACE economic activities classification); (ii) FIRE indicates the annual number of wildfires per region; BA in % denotes the annual burned area relative to the total area per region; (iii) CIs = confidence intervals.

recreation activities due to wildfires for the "Aracena y Picos de Aroche Natural Park" in Spain and show a susceptibility increase of 58 million euros due to travel and incidental costs. Moreover, Otrachshenko and Nunes (2022) estimate the effect of forest fires on tourist arrivals for 278 municipalities in Portugal and show that a 1% increase in BA in a given year reduces the tourist arrivals in that year by 3.5%.

The second significantly affected category, is the employment growth in NACE activity sections K–N, which include financial and insurance activities (e.g., risk and damage evaluation, financial leasing, reinsurance), real estate activities, professional, scientific and technical activities (e.g., legal and accounting services, architectural and engineering activities) as well as administrative and support service activities (e.g., renting and leasing of motor vehicles and construction machinery, temporary employment agencies activities, security and investigation activities, services to buildings and landscape activities). The magnitude of the effects indicate that wildfires lead to an increase in the regional annual employment growth in these sectors of 0.13–0.22% ($0.00308 * 7 = 0.022$) using fire numbers (Column (3)) and $1.695 * 0.0077 = 0.013$ using BA (Column (4)) conditional on a region having experienced at least one wildfire. The estimated positive employment effect in this NACE category seems sensible in response to wildfires, particularly as it incorporates insurance and damage evaluation, real estate activities, temporary employment activities (i.e., this includes short-term contracting possibly in the labour intensive construction sector or for additional firefighters), as well as services to buildings and landscapes activities which comprises cleaning of affected buildings and landscapes in the aftermaths of a wildfire.

On average 32,137 people (11.1%) work in sections K–N (see Table B3 in Appendix B) and thus a wildfire affected region experiences an annual increase of 42–71 jobs in this sector ($32,137 * 0.0013 = 42$ using BA and $32,137 * 0.0022 = 71$ using fire

Table 9
Wildfires and employment and GDP growth with lags (2011–2018).

	Δlog(EMP)			Δlog(GDP)		
	(1)	(2)	(3)	(4)	(5)	(6)
$FIRE_t \times 10^{-2}$	0.044	0.041	0.013	−0.259**	−0.259**	−0.222**
	(0.064)	(0.069)	(0.061)	(0.085)	(0.088)	(0.084)
$FIRE_{t-1} \times 10^{-2}$		0.089**	0.065		−0.009	−0.009
		(0.034)	(0.036)		(0.044)	(0.037)
$FIRE_{t-2} \times 10^{-2}$			0.057			−0.004
			(0.037)			(0.040)
BA_t	0.240	0.135	−0.040	−1.425**	−1.435**	−1.241**
	(0.354)	(0.382)	(0.347)	(0.468)	(0.477)	(0.444)
BA_{t-1}		0.524**	0.543**		0.052	0.171
		(0.193)	(0.207)		(0.260)	(0.210)
BA_{t-2}			0.208			0.130
			(0.208)			(0.191)

Notes: (i) * p <0.05, ** p <0.01; (ii) standard errors in parentheses are bootstrapped (1000 replications) and clustered on the regional level; (iii) N = 1864; (d) Δlog(EMP) denotes the growth in the employment rate and Δlog(GDP) is the GDP growth rate; $FIRE_t$ indicates the number of fires in year t (stated in 100 fires); BA_t is the proportion of the annual burned area per region in year t; (iv) all estimations are run with FWI controls that include the Fire Weather Index for predominantly urban and agricultural areas as well as for wetlands and water bodies; climate controls that include summer and annual means of the variables temperature, precipitation, relative humidity, and wind speed for each of the four land cover type categories separately; as well as fixed effects including regional and time fixed effects.

numbers). For an average fire season (i.e., 102 wildfire affected regions), this leads to an additional 4,284–7,242 jobs related to financial, insurance, real estate, as well as administrative and support service activities in Southern Europe.

4.3. Lagged impact

Wildfires might have a more sustained effect on regional economies. Therefore, we explore whether there are lagged effects on regional employment and GDP growth of wildfires by including two lags of the wildfire impact variables in Eq. (2). As noted earlier, the reported standard errors of all lagged estimations are not robust to spatial correlation, and thus must be interpreted relatively cautiously.

The results shown in Table 9 suggest consistently that it is only in the contemporary year that the GDP growth rate (Columns 4–6) is affected for both wildfire impact variables. In contrast, the results regarding the effect of BA on aggregate employment growth (and fire numbers for lag 1) indicate that there is a positive effect of the prior year. This would imply, subject to the concerns regarding the lack of spatial correlation taken account of in the standard errors, that a region's annual aggregate employment growth increases on average by 0.04–0.06% ($0.00089 * 7 = 0.006$ using fire numbers in Column (2), $0.524 * 0.0077 = 0.004$ using BA in Column (2), or $0.543 * 0.0077 = 0.004$ using BA in Column (3)) conditional on having experienced at least one wildfire. This aligns with recent research on the economic effects of natural disasters presented in Deryugina (2022) showing long-term labour market resilience for wealthy countries.

4.4. Robustness checks

To test the robustness of our baseline estimations, we conduct the Fisher randomisation test introduced by Fisher (1937) for the estimates of the wildfire impact variables on GDP growth. We randomly reshuffle the fire numbers and BA across space and time (keeping the instrument and the control variables fixed) and run the IV regressions performing 1000 iterations. The results displayed in Fig. 6 show the high level of significance of our results (indicated by the t-statistic of the actual estimate) with a p-value of 0.004 for both fire numbers and for BA. This demonstrates that our results are not driven by chance.

As described in Section 3, we choose 33 km as the distance cutoff for the spatially robust HAC standard errors since this reflected the median distance between regions' centroids. To explore how sensitive our results are to this choice we incrementally increase the threshold and re-estimate Eq. (2). Fig. 7 shows that the spatial standard errors increase in distance and become insignificant after we choose values of approximately 40 to 140 kilometres for the BA and fire numbers, respectively. Thus, our findings are only robust to assuming that potential regional economic shocks or spillover effects are limited to mostly adjacent regions.

To explore a potential economic impact beyond the directly affected BA we create buffers of one and five kilometres around each wildfire BA polygon. The underlying idea is to evaluate whether the effects extend to surrounding areas given those arguably suffer from indirect impacts (e.g., road closures, business downtime, decrease in tourism). Similar to the baseline estimations, we find significant negative effects of the wildfire impact variables on the GDP growth rate and insignificant positive effects on employment growth for the buffered estimations. The magnitude of the coefficient decreases with increasing buffer size as shown in Table 10.

Finally, one might be concerned that migration potentially impacts our findings. As explained in Section 3 we implement spatial standard errors, robust to various cutoffs between 40 to 140 kilometres, in our main estimations. This would take account of migration into neighbouring regions as long as these act through shocks captured in the error term. We additionally run our

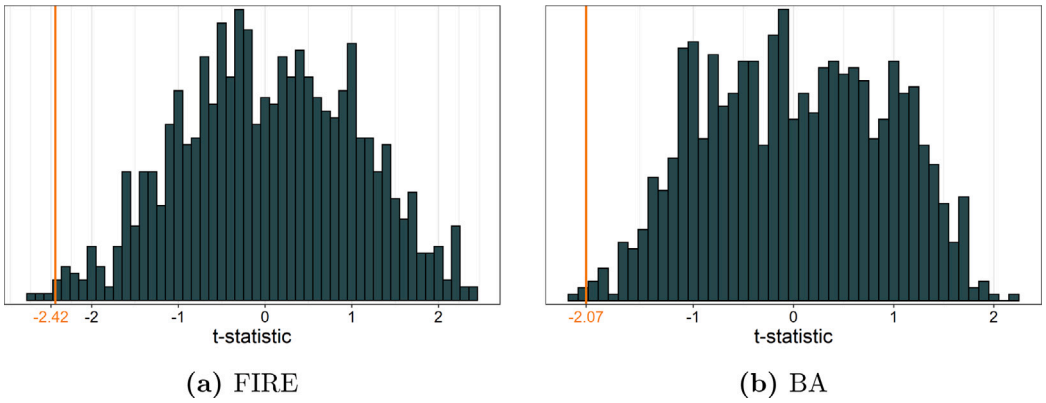

Fig. 6. Fisher randomisation test of wildfire impact variables and GDP growth with 1000 iterations.
Notes: (i) the vertical line indicates the t-statistic of our actual estimate; (ii) FIRE indicates the annual number of wildfires per region; BA in % denotes the annual burned area relative to the total area per region.

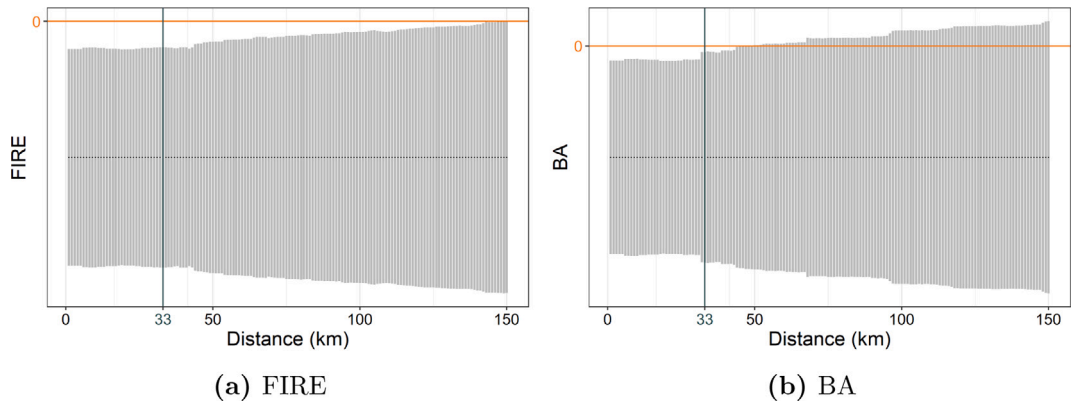

Fig. 7. Spatial HAC standard errors with varying distance cutoff estimating the wildfire impact on GDP growth.
Notes: (i) the vertical line indicates the selected cutoff value of 33 km; (ii) FIRE indicates the annual number of wildfires per region; BA in % denotes the annual burned area relative to the total area per region.

Table 10
Wildfires and employment and GDP growth with buffered estimations (2011–2018).

	Direct	Buffer 1 km	Buffer 5 km
Δlog(EMP)			
FIRE $\times 10^{-2}$	0.044	0.016	0.001
BA	0.240	0.088	0.012
Δlog(GDP)			
FIRE $\times 10^{-2}$	−0.259*	−0.093*	−0.007*
BA	−1.425*	−0.522*	−0.070*

Notes: (i) * p <0.05; (ii) direct effects incorporate the actual burned area; for potential effects beyond the burned area, buffers of size 1 and 5 km area created around each polygon; (iii) Δlog(EMP) denotes the growth of the employment rate; Δlog(GDP) is the per capita GDP growth rate; FIRE is annual number of fires per region (in 100 fires); BA is the proportion of the annual burned area per region; (iv) climate controls include summer and annual means of the variables temperature, precipitation, relative humidity, and wind speed for each of the four land cover type categories separately; FWI controls include the Fire Weather Index for predominantly urban and agricultural areas as well as for wetlands and water bodies; fixed effects include regional and time fixed effects.

specification in Eq. (2) but using regional population growth as the dependent variable. More precisely, as long as births and deaths are not directly affected by wildfires, or their effects cancel each other out, or in net are less than any effect on migration, then any impact on population growth can be considered to be due to net migration. However, the results of this exercise showed that neither the reduced form (coefficient 0.00; standard error 0.00) nor the IV estimates for fire numbers (coefficient 0.007; standard

error 0.008) and BA (coefficient 0.039; standard error 0.045) were significant. Thus, either there is no effect on net migration or the effect is cancelled out by impacts of the birth net of the death rate.

Nevertheless, we need to emphasise that our study estimates the aggregated effects of all wildfire occurrences per region and year, most of which are arguably not disastrous. This is in strong contrast to the existing migration literature in the natural hazards context that sets a focus on large-scale devastating events (Karácsonyi et al., 2021).[28] For example, Sheldon and Zhan (2022) find county out-migration following hurricanes and floods using Federal Emergency Management Agency (FEMA) data. Regarding wildfires, Winkler and Rouleau (2021) suggest that extreme wildfires (as declared by FEMA) in the US may be associated with out-migration. Similarly, Boustan et al. (2020) report increased out-migration for severe fire events using FEMA data from 1920 to 2010 in the US, although it needs to be pointed out that in their specification a severe fire event is associated with at least 25 moralities. Out of the more than 6000 wildfires in our dataset, less than a hand full would be categorised accordingly.

There are reasons why residents are unlikely to migrate after being affected by a wildfire. For instance, areas that are fire-prone often simultaneously draw people due to their intrinsic environmental amenities, as extensively outlined in McConnell et al. (2021). More precisely, even for large and devastating wildfires, the negative impact may not be big enough to outweigh the amenity-draw to that very place. Evidence in line with this notion shows that even for disastrous wildfire events, such as the California's 2017 North Bay fires which resulted in more than 6000 structures damaged or destroyed, a small minority of affected households moved out of the county (Sharygin, 2021). Finally, a recent study by McConnell et al. (2021) investigates fires that are known to have destroyed at least one building, i.e., 16% of fires in their sample, and find in-as well as out-migration for the entire sample and an increase in out-migration for fires that destroyed more than 17 buildings. The authors state as a broader conclusion that residents largely remain in fire-prone regions after less destructive events, which per definition are arguably more destructive than the majority of fires in our data set.

5. Conclusions

In this paper we link high resolution satellite data of aggregate wildfire burned areas with regional economic data for Southern Europe, enabling us to contribute to a deeper understanding of how these events impact local economic outcomes. Given that wildfire incidents are likely correlated with various unobservable factors, such as land management policies, wildfire prevention strategies, and land-use changes, and can be set intentionally, the events are treated as endogenous in our analysis. To overcome this concern we use a measure of wildfire occurrence probability for predominantly forested areas based on relevant climatic features as an instrumental variable, while controlling for fire danger in non-forested area as well as for general climatic conditions that might directly affect regional economies. Importantly, the analysis indicates that not taking account of the endogeneity of wildfires is likely to lead to biased estimates on economic impacts. The proposed instrumental variable strategy might thus also prove to be a useful approach for other researchers interested in the economic implications of wildfires.

Our causally identified results for Southern Europe show a consistent negative contemporary effect of wildfires on the annual regional GDP growth rate ranging from 0.11 to 0.18%. For the most severe wildfire years, the effect can lead to a decrease in the GDP growth rate of approximately 3.3–4.8% using fire numbers and burned area, respectively. The disaggregated employment analysis by economic activity categories reveals heterogeneous impacts, where industries such as wholesale and retail trade, transport, accommodation and food service activities are experiencing a negative employment effect of 0.09–0.15%, plausibly as a result of disruptions related to tourism. In contrast, our results show a positive effect of wildfires on regional employment growth of 0.13–0.22% in sectors including financial, insurance, and real estate activities, as well as short-term contracting activities.

Overall our study provides novel evidence that wildfires lead to a significant decrease in the regional GDP growth rate for Southern Europe. Although wildfires have formed an integral part of the Mediterranean landscapes for centuries, the public institutional response could benefit from an extensive evaluation of mitigation and prevention mechanisms (e.g., mechanical clearing, prescribed burning, grazing, land management activities) to reduce the negative impacts on local economies. As illustrated in Bayham et al. (2022), economic interdependencies and inefficiencies in fire-prone landscapes render wildfire management highly complex and large research gaps remain. European wide data collection efforts on these aspects at the regional level would allow researchers to further investigate the possible role of these interventionist factors. Such insights would importantly allow regional policy makers to explicitly evaluate strategies to strengthen the resilience of regional economies, particularly since the potential damage of wildfires is predicted to become more pronounced in the future (Dupuy et al., 2020).

Declaration of competing interest

The authors declare that they have no known competing financial interests or personal relationships that could have appeared to influence the work reported in this paper.

[28] We hereby focus on studies looking at revealed preferences and do not discuss publications studying stated preferences (e.g., surveys quantifying the intention to move after severe wildfire events) such as Nawrotzki et al. (2014) or Berlin Rubin and Wong-Parodi (2022).

Appendix A. Fire weather index equations

Given the complexity of the FWI calculations, we limit ourselves to illustrate the derivations of the direct fire behaviour inputs to the FWI, which are the Initial Spread Index (ISI) and the Buildup Index (BUI). Thus, we will not elude to the underlying functions of the respective inputs, namely the function of wind $f(W)$, the fine fuel moisture function $f(F)$, today's Duff Moisture Code denoted as P, and today's Drought Code denoted as D. The exposition of the exact equations here forth strongly draws on Van Wagner and Pickett (1985), where the full set of equations based on the primary input variables is described.

The Initial Spread Index is defined by Eq. (3), whereby $f(W)$ is a function of wind and $f(F)$ is the fine fuel moisture function.

$$\text{ISI} = 0.208 * f(W) * f(F) \tag{3}$$

The Buildup Index shown in Eq. (4) is a function of today's Duff Moisture Code (DMC) denoted as P and today's Drought Code (DC) denoted as D.

$$\text{BUI} = \begin{cases} 0.8 * PD/(P + 0.4 * D), & \text{if } P \leq 0.4 * D \\ \text{P} - [1 - 0.8 * D/(P + 0.4 * D)][0.92 + (0.0114 * P)^{1.7}], & \text{if } P > 0.4 * D \end{cases} \tag{4}$$

The output of Eq. (4) is subsequently used as input to calculate the duff moisture function, $f(D)$, shown in Eq. (5).

$$f(D) = \begin{cases} 0.626 * \text{BUI}^{0.809} + 2, & \text{if BUI} \leq 80 \\ 1000(25 + 108.64e^{-0.023*\text{BUI}}), & \text{if BUI} > 80 \end{cases} \tag{5}$$

Eq. (6) derives B, which is an intermediate form of the FWI, by scaling and multiplying today's ISI with the duff moisture function.

$$B = 0.1 * \text{ISI} * f(D) \tag{6}$$

Finally, Eq. (7) shows the derivation of the FWI in its final form.

$$\text{FWI} = \begin{cases} B, & \text{if B} \leq 1 \\ 2.72(0.434 * ln(B))^{0.647}, & \text{if } B > 1 \end{cases} \tag{7}$$

Appendix B. Supplementary data

Supplementary material related to this article can be found online at https://doi.org/10.1016/j.jeem.2023.102787.

References

Alix-Garcia, J., Millimet, D.L., 2021. Remotely Incorrect? Accounting for nonclassical measurement in satellite data on deforestation.

Barattieri, A., et al., 2021. The short-run, dynamic employment effects of natural disasters: New insights. Working Paper ISSN 2292-0838, In: 2021s-22, CIRANO.

Barone, G., Mocetti, S., 2014. Natural disasters, growth and institutions: A tale of two earthquakes. J. Urban Econ. 84, 52–66.

Bayham, J., Yoder, J.K., Champ, P.A., Calkin, D.E., 2022. The economics of wildfire in the United States. Ann. Rev. Resour. Econ. 14.

Baylis, P., Boomhower, J., 2019. Moral Hazard, Wildfires, and the Economic Incidence of Natural Disasters (No. W26550). National Bureau of Economic Research.

Berlin Rubin, N., Wong-Parodi, G., 2022. As California Burns: The Psychology of Wildfire- and Wildfire Smoke-Related Migration Intentions. Springer Netherlands, pp. 15–45.

Borgschulte, M., Molitor, D., Zou, Z.Y., 2020. Air pollution and the labor market: Evidence from wildfire smoke. NBER Working Paper, pp. 1–47.

Botzen, W.J., Deschenes, O., Sanders, M., 2019. The economic impacts of natural disasters: A review of models and empirical studies. Rev. Environ. Econ. Policy 13 (2), 167–188.

Boustan, L.P., Kahn, M.E., Rhode, P.W., Yanguas, M.L., 2020. The effect of natural disasters on economic activity in US counties: A century of data. J. Urban Econ. 118, 103257.

Burke, M., et al., 2020. The changing risk and burden of wildfire in te US. In: NBER Working Paper Series, No. 27423.

Butry, D.T., et al., 2001. What is the price of catastrophic wildfire? J. Forestry 99 (11), 9–17.

Camia, A., Amatulli, G., San-Miguel-Ayanz, J., 2008. Past and future trends of forest fire danger in Europe. Technical Report March 2015, Joint Research Centre.

CCST, 2020. The costs of wildfire in California an independent review of scientific and technical information. Technical report, California Council on Science and Technology, Sacramento, California, p. 248.

Cliff, A., Ord, K., 1972. Testing for spatial autocorrelation among regression residuals. Geogr. Anal. 4 (3), 267–284.

Cornes, R.C., van der Schrier, G., van den Besselaar, E.J., Jones, P.D., 2018. An ensemble version of the E-OBS temperature and precipitation data sets. J. Geophys. Res.: Atmos. 123 (17), 9391–9409.

Damania, R., Desbureaux, S., Zaveri, E., 2020. Does rainfall matter for economic growth? Evidence from global sub-national data (1990–2014). J. Environ. Econ. Manag. 102, 102335.

Davis, E.J., Moseley, C., Nielsen-Pincus, M., Jakes, P.J., 2014. The community economic impacts of large wildfires: A case study from Trinity county, California. Soc. Nat. Resour. 27 (9), 983–993.

Deryugina, T., 2022. Economic effects of natural disasters. IZA World of Labor, pp. 1–10.

Deryugina, T., Kawano, L., Levitt, S., 2018. The economic impact of hurricane Katrina on its victims: Evidence from individual tax returns. Am. Econ. J.: Appl. Econ. 10 (2), 202–233.

Dupuy, J.-l., et al., 2020. Climate change impact on future wildfire danger and activity in Southern Europe: A review. Ann. Forest Sci. 77 (35).

European Environment Agency, 2021. CORINE land cover - User manual. Copernicus Land Monitoring Service 1.0, 128.

Eurostat, 2008. NACE Rev. 2 – Statistical classification of economic activities in the European community. Technical report, European Union, pp. 1–363.

Eurostat, 2013a. European system of accounts ESA 2010. Technical report, Publications Office of the European Union, European Comission, Luxembourg, p. 652.

Eurostat, 2013b. Manual on regional accounts methods. Technical report, European Commission, Luxembourg, p. 138.

Eurostat, 2020. Statistical regions in the European Union and partner countries, Technical report, 2020 European Union, Luembourg, pp. 1–188.

Felbermayr, G., Gröschl, J., 2014. Naturally negative: The growth effects of natural disasters. J. Dev. Econ. 111, 92–106.
Fisher, R.A., 1937. The Design of Experiments, second ed. Oliver & Boyd, Edinburgh & London.
Fomby, T., Ikeda, Y., Loayza, N., 2013. The growth aftermath of natural disasters. J. Appl. Econometrics 28, 412–434.
Foreman, T., 2020. SPATIAL_HAC_IV: Stata module to estimate an instrumental variable regression, adjusting standard errors for spatial correlation, heteroskedasticity, and autocorrelation. Statistical Software Components S458872, Boston College Department of Economics.
Garcia, A., Heilmayr, R., 2022. Conservation impact evaluation using remotely sensed data. Available at SSRN 4179782.
Gellman, J., Walls, M., Wibbenmeyer, M., 2022. Wildfire, smoke, and outdoor recreation in the Western United States. Forest Policy Econ. 134, 102619.
Groen, J.A., Kutzbach, M.J., Polivka, A.E., 2020. Storms and jobs: The effect of hurricanes on individuals' employment and earnings over the long term. J. Labor Econ. 38 (3), 653–685.
Hersbach, H., et al., 2020. The ERA5 global reanalysis. Q. J. R. Meteorol. Soc. 146 (730), 1999–2049.
Holmes, T.P., Prestemon, J.P., Abt, K.L., 2008. An Introduction to the Economics of Forest Disturbance. Springer, pp. 3–14.
Horwich, G., 2000. Economic lessons of the Kobe earthquake. Econom. Dev. Cult. Chang. 48 (3), 521–542.
Iammarino, S., Rodriguez-Pose, A., Storper, M., 2019. Regional inequality in Europe: Evidence, theory and policy implications. J. Econ. Geogr. 19 (2), 273–298.
Johnston, F.H., et al., 2021. Unprecedented health costs of smoke-related PM2.5 from the 2019–20 Australian megafires. Nat. Sustain. 4 (1), 42–47.
Karácsonyi, D., Taylor, A., Bird, D., 2021. The Demography of Disasters: Impacts for Population and Place. Springer Nature.
Kim, M.K., Jakus, P.M., 2019. Wildfire, national park visitation, and changes in regional economic activity. J. Outdoor Recreat. Tourism 26, 34–42.
Klomp, J., Valckx, K., 2014. Natural disasters and economic growth: A meta-analysis. Global Environ. Change 26 (1), 183–195.
Kochi, I., Champ, P.A., Loomis, J.B., Donovan, G.H., 2012. Valuing mortality impacts of smoke exposure from major Southern California wildfires. J. Forest Econ. 18 (1), 61–75.
Kramer, H.A., Butsic, V., Mockrin, M.H., Ramirez-Reyes, C., Alexandre, P.M., Radeloff, V.C., 2021. Post-wildfire rebuilding and new development in California indicates minimal adaptation to fire risk. Land Use Policy 107, 105502.
Loayza, N.V., Olaberría, E., Rigolini, J., Christiaensen, L., 2012. Natural disasters and growth: Going beyond the averages. World Dev. 40 (7), 1317–1336.
McCaffrey, S., 2004. Thinking of wildfire as a natural hazard. Soc. Nat. Resour. 17 (6), 509–516.
McConnell, K., et al., 2021. Effects of wildfire destruction on migration, consumer credit, and financial distress. Federal Reserve Bank of Cleveland Working Paper No. 21-29, Federal Reserve Bank of Cleveland.
McCoy, S.J., Walsh, R.P., 2018. Wildfire risk, salience & housing demand. J. Environ. Econ. Manag. 91, 203–228.
McElhinny, M., et al., 2020. A high-resolution reanalysis of global fire weather from 1979 to 2018 - Overwintering the drought code. Earth Syst. Sci. Data 12 (3), 1823–1833.
Michetti, M., Pinar, M., 2019. Forest fires across Italian regions and implications for climate change: A panel data analysis. Environ. Resour. Econ. 72 (1), 207–246.
Molina, J.R., González-Cabán, A., Rodríguez y Silva, F., 2019. Wildfires impact on the economic susceptibility of recreation activities: Application in a Mediterranean protected area. J. Environ. Manag. 245, 454–463.
Moran, P., 1950. Notes on continuous stochastic phenomena. Biometrika 37 (1), 17–23.
Morton, D.C., Roessing, M.E., Camp, A.E., Tyrrell, M.L., 2003. Assessing the Environmental, Social, and Economic Impacts of Wildfire. Global institute of Sustainable Forestry, New Haven, Connecticut.
Mueller, J.M., Loomis, J.B., 2014. Does the estimated impact of wildfires vary with the housing price distribution? A quantile regression approach. Land Use Policy 41, 121–127.
Naguib, C., Pelli, M., Poirier, D., Tschopp, J., 2022. The impact of cyclones on local economic growth: Evidence from local projections. CIRANO Working Paper, 26.
Nawrotzki, R.J., Brenkert-Smith, H., Hunter, L.M., Champ, P.A., 2014. Wildfire-migration dynamics: Lessons from Colorado's Fourmile Canyon fire. Soc. Nat. Resour. 27 (2), 215–225.
Nicholls, S., 2019. Impacts of environmental disturbances on housing prices: A review of the hedonic pricing literature. J. Environ. Manag. 246, 1–10.
Nielsen-Pincus, M., Moseley, C., Gebert, K., 2013. The effects of large wildfires on employment and wage growth and volatility in the Western United States. J. Forestry 111 (6), 404–411.
Nielsen-Pincus, M., Moseley, C., Gebert, K., 2014. Job growth and loss across sectors and time in the Western US: The impact of large wildfires. Forest Policy Econ. 38, 199–206.
Otrachshenko, V., Nunes, L.C., 2022. Fire takes no vacation: Impact of fires on tourism. Environ. Dev. Econ. 27 (1), 86–101.
Parida, Y., Saini, S., Chowdhury, J.R., 2021. Economic growth in the aftermath of floods in Indian states. Environ. Dev. Sustain. 23 (1), 535–561.
Rego, F., Louro, G., Constantino, L., 2013. The impact of changing wildfire regimes on wood availability from Portuguese forests. Forest Policy Econ. 29, 56–61.
Richardson, L.A., Champ, P.A., Loomis, J.B., 2012. The hidden cost of wildfires: Economic valuation of health effects of wildfire smoke exposure in Southern California. J. Forest Econ. 18 (1), 14–35.
San-Miguel-Ayanz, J., et al., 2021. Forest fires in Europe, Middle East and North Africa 2020. Technical report, Joint Research Centre, Luxembourg.
San-Miguel-Ayanz, J., et al., 2022. Forest fires in Europe, Middle East and North Africa 2021. Technical report, Joint Research Centre, Luxembourg.
Sharygin, E., 2021. Estimating migration impacts of wildfire: California's 2017 North Bay fires. In: The Demography of Disasters. Springer, pp. 49–70.
Sheldon, T.L., Zhan, C., 2022. The impact of hurricanes and floods on domestic migration. J. Environ. Econ. Manag. 115, 102726.
Skouras, S., Christodoulakis, N., 2014. Electoral misgovernance cycles: Evidence from wildfires and tax evasion in Greece. Public Choice 159 (3), 533–559.
Stephenson, C., Handmer, J., Robyn, B., 2013. Estimating the economic, social and environmental impacts of wildfires in Australia. Environ. Hazards 12 (2), 93–111.
Stock, J.H., Wright, J.H., Yogo, M., 2002. A survey of weak instruments and weak identification in generalized method of moments. J. Bus. Econom. Statist. 20 (4), 518–529.
Strobl, E., 2011. The economic growth impact of hurricanes: Evidence from U.S. coastal counties. Rev. Econ. Stat. 93 (2), 575–589.
Sullivan, A., Baker, E., Kurvits, T., 2022. Spreading like wildfire: The rising threat of extraordinary landscape fires. In: A UNEP Rapid Response Assessment. Nairobi. UNEP: United Nations Environment Programme.
Tarín-Carrasco, P., et al., 2021. Impact of large wildfires on PM10 levels and human mortality in Portugal. Nat. Hazards Earth Syst. Sci. 21 (9), 2867–2880.
Van Wagner, C.E., Pickett, T.L., 1985. Equations and FORTRAN program for the Canadian forest fire weather index system. Technical report, Canadian Forestry Service, Ottawa.
Wang, D., et al., 2021. Economic footprint of California wildfires in 2018. Nat. Sustain. 4 (3), 252–260.
Winkler, R.L., Rouleau, M.D., 2021. Amenities or disamenities? Estimating the impacts of extreme heat and wildfire on domestic US migration. Popul. Environ. 42 (4), 622–648.